

C–H Bond Activation of Benzene and Methane by $M(\eta^2\text{-O}_2\text{CH})_2$ ($M = \text{Pd}$ or Pt). A Theoretical Study

Bishajit Biswas, Manabu Sugimoto, and Shigeyoshi Sakaki*

Department of Applied Chemistry and Biochemistry, Faculty of Engineering,
Kumamoto University, Kurokami, Kumamoto 860-8555, Japan

Received January 3, 2000

C–H bond activations of benzene and methane by $M(\eta^2\text{-O}_2\text{CH})_2$ ($M = \text{Pd}$ or Pt) are theoretically investigated with density functional theory (DFT), MP2-MP4(SDQ), and CCSD(T) methods. The C–H bond activation of benzene takes place with activation energies (E_a) of 16.1 and 21.2 kcal/mol and reaction energies (ΔE) of -16.5 and -25.8 kcal/mol for $M = \text{Pd}$ and Pt , respectively, to afford $M(\eta^2\text{-O}_2\text{CH})(\text{C}_6\text{H}_5)(\eta^1\text{-HCOOH})$, where MP4(SDQ) values are given hereafter and a negative ΔE value represents that the reaction is exothermic. The C–H bond activation of methane proceeds with E_a values of 21.5 and 17.3 kcal/mol and ΔE values of -8.3 and -13.3 kcal/mol for $M = \text{Pd}$ and Pt , respectively, to afford $M(\eta^2\text{-O}_2\text{CH})\text{-}(\text{CH}_3)(\eta^1\text{-HCOOH})$. However, C–H bond activations of benzene and methane by $\text{Pd}(\text{PH}_3)_2$ need a large E_a value, and these reactions are significantly endothermic: $E_a = 26.5$ kcal/mol and $\Delta E = 22.1$ kcal/mol for benzene and $E_a = 34.7$ kcal/mol and $\Delta E = 31.5$ kcal/mol for methane. Also, the C–H bond activation of methane by $\text{Pt}(\text{PH}_3)_2$ needs a large E_a value (28.1 kcal/mol) with moderate endothermicity ($\Delta E = 7.0$ kcal/mol), while the C–H bond activation of benzene by $\text{Pt}(\text{PH}_3)_2$ occurs with a moderate E_a value (17.3 kcal/mol) and a negative ΔE value (-3.9 kcal/mol). From these results, the following conclusions are presented: (1) $\text{Pd}(\eta^2\text{-O}_2\text{CH})_2$ can perform easily the C–H bond activations of benzene and methane but $\text{Pd}(\text{PH}_3)_2$ cannot. This is because the formate ligand assists the C–H bond activation through formation of a strong O–H bond. (2) $\text{Pt}(\eta^2\text{-O}_2\text{CH})_2$ more easily performs the C–H bond activation of methane but much less easily the C–H bond activation of benzene than $\text{Pd}(\eta^2\text{-O}_2\text{CH})_2$, because the intermediate, $\text{Pt}(\text{II})$ –benzene complex, is too stable. (3) Benzene more easily undergoes C–H bond activation than does methane. The higher reactivity of benzene is interpreted in terms of $M\text{-C}_6\text{H}_5$ and $M\text{-CH}_3$ bond energies and the bonding interaction of benzene π and π^* orbitals with M d orbitals. Analysis of electron distribution implicitly indicates that the C–H bond activation by $M(\eta^2\text{-O}_2\text{CH})_2$ is characterized to be heterolytic C–H bond fission, while the C–H bond activation by $M(\text{PH}_3)_2$ is characterized to be homolytic C–H bond fission.

Introduction

Functionalization of alkane and aromatic compounds through C–H bond activation by transition metal complexes is one of the most important subjects of research in organometallic chemistry.¹ In this regard, many experimental^{2–21} and many theoretical works^{22–30} have been reported on homolytic C–H bond activation. Also, many experimental works^{31–48} and rather limited theoretical works^{49,50} have been presented on heterolytic C–H bond activation. Here, we use the term “homolytic

C–H bond activation” to represent the C–H bond fission by the oxidative addition to a low-valent transition

- (1) (a) Shilov, A. E. *Activation of Saturated Hydrocarbons by Transition Metal Complexes*; D. Reidel: Boston, MA, 1984. (b) Crabtree, R. H. *Chem. Rev.* **1985**, *85*, 245. (c) Ryabov, A. D. *Chem. Rev.* **1990**, *90*, 403. (d) Shilov, A. E.; Shulpin, B. G. *Chem. Rev.* **1997**, *97*, 2879. (2) (a) Gianotti, C.; Green, M. L. H. *J. Chem. Soc., Chem. Commun.* **1972**, 1114. (b) Green, M. L. H. *Pure Appl. Chem.* **1978**, *50*, 27. (3) (a) Crabtree, R. H.; Miheleic, J. M.; Quirk, J. M. *J. Am. Chem. Soc.* **1979**, *101*, 7738. (b) Crabtree, R. H.; Holt, E. M.; Lavin, M.; Morehouse, S. M. *Inorg. Chem.* **1985**, *24*, 1986. (c) Crabtree, R. H. *Angew. Chem., Int. Ed. Engl.* **1993**, *32*, 289. (4) (a) Hoyano, J. K.; Graham, W. A. *J. Am. Chem. Soc.* **1982**, *104*, 3723. (b) Hoyano, J. K.; McMaster, A. D.; Graham, W. A. *J. Am. Chem. Soc.* **1983**, *105*, 7190. (c) Rest, A. J.; Whitwell, I.; Graham, W. A. G.; Hoyano, J. K.; McMaster, A. D. *J. Chem. Soc., Chem. Commun.* **1984**, 624.

- (5) (a) Janowicz, A. H.; Bergman, R. G. *J. Am. Chem. Soc.* **1982**, *104*, 352; **1983**, *105*, 3929. (b) Wax, M. J.; Kovac, C. A.; Bergman, R. G. *J. Am. Chem. Soc.* **1984**, *106*, 1121. (c) Bergman, R. G. *Science* **1984**, *223*, 902. (d) Mcghee, W. D.; Hollander, F. J.; Bergman, R. G. *J. Am. Chem. Soc.* **1988**, *110*, 8428. (e) Bergman, R. G. *J. Organomet. Chem.* **1990**, *400*, 273. (f) Arndtsen, B. A.; Bergman, R. G.; Mobley, T. A.; Peterson, T. H. *Acc. Chem. Res.* **1995**, *28*, 154. (g) Lian, T.; Bromberg, S. E.; Yang, H.; Proulx, G.; Bergman, R. G.; Harris, C. B. *J. Am. Chem. Soc.* **1996**, *118*, 3769. (6) (a) Jones, W. D.; Feher, F. J. *J. Am. Chem. Soc.* **1982**, *104*, 4240; **1986**, *108*, 4841; *Organometallics* **1983**, *2*, 562. (b) Jones, W. D.; Feher, F. J. *Acc. Chem. Res.* **1989**, *22*, 91. (c) Wick, D. D.; Jones, W. D. *Organometallics* **1999**, *18*, 495. (7) (a) Hackett, M.; Ibers, J. A.; Jernakoff, P.; Whitesides, G. M. *J. Am. Chem. Soc.* **1986**, *108*, 8094. (b) Hackett, M.; Whitesides, G. M. *J. Am. Chem. Soc.* **1988**, *110*, 1449. (8) (a) Sakakura, T.; Tanaka, M. *Chem. Lett.* **1987**, *249*, 1113. (b) Sakakura, T.; Sodeyama, T.; Sasaki, K.; Wada, K.; Tanaka, M. *J. Am. Chem. Soc.* **1990**, *112*, 7221. (9) Magire, J. A.; Boese, W. T.; Goldman, A. S. *J. Am. Chem. Soc.* **1989**, *111*, 7088. (10) Rabinovich, D.; Parkin, G. *J. Am. Chem. Soc.* **1990**, *112*, 5381. (11) Mizuko, Y.; Kasuga, N.; Komiya, S. *Chem. Lett.* **1991**, 2127. (12) Bianchini, C.; Barbaro, P.; Meli, A.; Peruzzini, M.; Vacca, A.; Vizza, F. *Organometallics* **1993**, *12*, 2505. (13) Perutz, R. N. *Chem. Soc. Rev.* **1993**, 361.

metal complex to afford a transition metal alkyl (or aryl) hydride complex (eq 1) and the term "heterolytic C–H bond activation" to represent the C–H bond fission by a transition metal complex to afford a transition metal alkyl (or aryl) complex and HX (eq 2).



(R = C₆H₅ or CH₃; X = an anionic ligand)

In the former reaction, the oxidation state of metal formally increases by 2, while it does not change in the latter reaction.

(14) (a) Murai, S.; Kakiuchi, F.; Sekine, S.; Tanaka, Y.; Kamatani, A.; Sonoda, M.; Chatani, N. *Nature* **1993**, *366*, 529. (b) Murai, S.; Kakiuchi, F.; Sekine, S.; Tanaka, Y.; Kamatani, A.; Sonoda, M.; Chatani, N. *Pure Appl. Chem.* **1994**, *66*, 1527. (c) Kakiuchi, F.; Sekine, S.; Tanaka, Y.; Kamatani, A.; Sonoda, M.; Chatani, N.; Murai, S. *Bull. Chem. Soc. Jpn.* **1995**, *68*, 62. (d) Murai, S.; Chatani, N.; Kakiuchi, F. *Pure Appl. Chem.* **1997**, *69*, 589. (e) Chatani, N.; Morimoto, T.; Fukumoto, Y.; Murai, S. *J. Am. Chem. Soc.* **1998**, *120*, 5335.

(15) Yamamoto, Y.; Al-masum, M.; Asao, N. *J. Am. Chem. Soc.* **1994**, *116*, 6019. (b) Yamamoto, Y.; Al-masum, M.; Fujiwara, N.; Asao, N. *Tetrahedron Lett.* **1995**, *36*, 2811.

(16) Blum, O.; Milstein, D. *J. Am. Chem. Soc.* **1995**, *117*, 4582.

(17) Murahashi, S.-I.; Naota, T.; Taki, H.; Mizuno, M.; Takaya, H.; Komiya, S.; Mizuno, Y.; Oyasato, N.; Hiraoka, M.; Hirano, M.; Fukuoka, A. *J. Am. Chem. Soc.* **1995**, *117*, 12436. (b) Murahashi, S.-I.; Naota, T. *Bull. Chem. Soc. Jpn.* **1996**, *69*, 1805.

(18) Purwoko, A. A.; Lees, A. *J. Inorg. Chem.* **1996**, *35*, 675.

(19) (a) Paneque, M.; Taboada, S.; Carmona, E. *Organometallics* **1996**, *15*, 2678. (b) Gutierrez-Puebla, E.; Monge, A.; Nicasio, M. C.; Perez, P. J.; Poveda, M. L.; Rey, L.; Ruiz, C.; Carmona, E. *Inorg. Chem.* **1998**, *37*, 4538. (c) Paneque, M.; Poveda, M. L.; Salazar, V.; Taboada, S.; Carmona, E. *Organometallics* **1999**, *18*, 139.

(20) Wick, D. D.; Jones, W. D. *Organometallics* **1999**, *18*, 495.

(21) Tobita, H.; Hashidzume, K.; Endo, K.; Ogino, H. *Organometallics* **1998**, *17*, 3406.

(22) Saillard, J.-Y.; Hoffmann, R. *J. Am. Chem. Soc.* **1984**, *106*, 2006.

(23) (a) Obara, S.; Kitaura, K.; Morokuma, K. *J. Am. Chem. Soc.* **1984**, *106*, 7482. (b) Koga, N.; Morokuma, K. *J. Am. Chem. Soc.* **1990**, *94*, 5454. (c) Koga, N.; Morokuma, K. *J. Am. Chem. Soc.* **1993**, *115*, 6883. (d) Matsubara, T.; Koga, N.; Musaev, D. G.; Morokuma, K. *J. Am. Chem. Soc.* **1998**, *120*, 12692.

(24) (a) Low, J. J.; Goddard, W. A. *J. Am. Chem. Soc.* **1986**, *108*, 6115. (b) Low, J. J.; Goddard, W. A. *Organometallics* **1986**, *5*, 609.

(25) (a) Blomberg, M. R. A.; Siegbahn, P. E. M.; Nagashima, U.; Wennerberg, J. *J. Am. Chem. Soc.* **1991**, *113*, 424. (b) Svensson, M.; Blomberg, M. R. A.; Siegbahn, P. E. M. *J. Am. Chem. Soc.* **1991**, *113*, 7076. (c) Blomberg, M. R. A.; Siegbahn, P. E. M.; Svensson, M. *J. Am. Chem. Soc.* **1992**, *114*, 6095. (d) Siegbahn, P. E. M.; Blomberg, M. R. A.; Svensson, M. *J. Am. Chem. Soc.* **1993**, *115*, 4191. (e) Blomberg, M. R. A.; Siegbahn, P. E. M.; Svensson, M. *J. Phys. Chem.* **1994**, *98*, 2062. (f) Siegbahn, P. E. M.; Blomberg, M. R. A. *Organometallics* **1994**, *13*, 354. (g) Siegbahn, P. E. M. *Organometallics* **1994**, *13*, 2833. (h) Siegbahn, P. E. M.; Svensson, M. *J. Am. Chem. Soc.* **1994**, *116*, 10124. (i) Siegbahn, P. E. M. *J. Am. Chem. Soc.* **1996**, *118*, 1487. (j) Siegbahn, P. E. M.; Carlbtree, R. H. *J. Am. Chem. Soc.* **1996**, *118*, 4442.

(26) Song, J.; Hall, M. B. *Organometallics* **1993**, *12*, 3118. (b) Jimenez-Catao, R.; Hall, M. B. *Organometallics* **1996**, *15*, 1889. (c) Niu, S.-Q.; Hall, M. B. *J. Am. Chem. Soc.* **1998**, *120*, 6169.

(27) (a) Sakaki, S.; Ieki, M. *J. Am. Chem. Soc.* **1993**, *115*, 2373. (b) Sakaki, S.; Biswas, B.; Sugimoto, M. *J. Chem. Soc., Dalton Trans.* **1997**, 803. (c) Sakaki, S.; Biswas, B.; Sugimoto, M. *Organometallics* **1998**, *17*, 1278.

(28) Hinderling, C.; Feichtinger, D.; Plattner, D. A.; Chen, P. *J. Am. Chem. Soc.* **1997**, *119*, 10793.

(29) Su, M.-D.; Chu, S.-Y. *J. Am. Chem. Soc.* **1997**, *119*, 5373.

(30) Espinosa-Garcia, J.; Corchado, J. C.; Truhlar, D. G. *J. Am. Chem. Soc.* **1997**, *119*, 9891.

(31) (a) Moritani, I.; Fujiwara, Y. *Tetrahedron Lett.* **1967**, 1119. (b) Fujiwara, Y.; Moritani, I.; Matsuda, M. *Tetrahedron Lett.* **1968**, 633. (c) Fujiwara, Y.; Takaki, K.; Taniguchi, Y. *Synlett* **1996**, 591, and references therein.

(32) Moynaha, E. B.; Popp, F. D.; Bernecke, W. F. *J. Organomet. Chem.* **1967**, *19*, 229.

(33) Garmett, J. L.; Hodges, R. J. *J. Am. Chem. Soc.* **1967**, *89*, 4546.

(34) Kasahara, A.; Izumi, T.; Maemura, M. *Bull. Chem. Soc. Jpn.* **1977**, *50*, 1878.

(35) Errington, J.; McDonald, W. S.; Shaw, B. L. *J. Chem. Soc., Dalton Trans.* **1980**, 2312.

Despite those many works, reports of C–H bond activation followed by functionalization of alkane and aromatic compounds have been limited.^{8,14,15,17,31,37,39,42} One of the interesting and pioneering examples is Pd(II)-catalyzed coupling reaction of benzene with alkene since this reaction is considered a prototype of functionalization of aromatic compounds through C–H bond activation.^{31a} Actually, similar reactions such as Pd(II)-catalyzed conversion of methane to carboxylic acid^{31c} and Pt(II)-catalyzed conversion of methane to methanol have been also reported so far.^{31c} All these reactions are supposed to involve the C–H bond activation by palladium(II) and platinum(II) complexes as a key elementary step. Recently, Fuchita and his collaborators isolated a σ -phenylpalladium(II) complex from benzene and palladium(II) acetate³⁶ⁿ and determined its structure by X-ray diffraction analysis.^{36w} Even with the direct detection and isolation of the σ -phenylpalladium(II) complex, details of this C–H bond activation are still ambiguous; for instance, no informa-

(36) (a) Hiraki, K.; Fuchita, Y.; Takakura, S. *J. Organomet. Chem.* **1981**, *210*, 273. (b) Fuchita, Y.; Hiraki, K.; Yamaguchi, T.; Maruta, T. *J. Chem. Soc., Dalton Trans.* **1981**, 2405. (c) Hiraki, K.; Fuchita, Y.; Takechi, K. *Inorg. Chem.* **1981**, *20*, 4316. (d) Fuchita, Y.; Hiraki, K.; Kage, Y. *Bull. Chem. Soc. Jpn.* **1982**, *55*, 955. (e) Fuchita, Y.; Hiraki, K.; Uchiyama, T. *J. Chem. Soc., Dalton Trans.* **1983**, 897. (f) Hiraki, K.; Fuchita, Y.; Matsumoto, Y. *Chem. Lett.* **1984**, 1947. (g) Hiraki, K.; Fuchita, Y.; Kage, Y. *J. Chem. Soc., Dalton Trans.* **1984**, 99. (h) Hiraki, K.; Fuchita, Y.; Nakashima, M.; Hiraki, H. *Bull. Chem. Soc. Jpn.* **1986**, *59*, 3073. (i) Fuchita, Y.; Hiraki, K.; Kamogawa, Y.; Suenaga, M. *J. Chem. Soc., Chem. Commun.* **1987**, 941. (j) Fuchita, Y.; Nakashima, M.; Hiraki, K.; Kawatani, M.; Ohnuma, K. *J. Chem. Soc., Dalton Trans.* **1988**, 785. (k) Fuchita, Y.; Hiraki, K.; Kamogawa, Y.; Suenaga, M.; Yohgoh, K.; Fujiwara, Y. *Bull. Chem. Soc. Jpn.* **1989**, *62*, 1081. (l) Hiraki, K.; Fuchita, Y. *Inorg. Synth.* **1989**, *26*, 208. (m) Fuchita, Y.; Akiyama, M. *Inorg. Chim. Acta* **1991**, *189*, 129. (n) Fuchita, Y.; Kawakami, M.; Shimoke, K. *Polyhedron* **1991**, *10*, 2037. (o) Hiraki, K.; Nakashima, M.; Uchiyama, T.; Fuchita, Y. *J. Organomet. Chem.* **1992**, *428*, 249. (p) Fuchita, Y.; Tsuchiya, H. *Inorg. Chim. Acta* **1993**, *209*, 229. (q) Fuchita, Y.; Tsuchiya, H. *Polyhedron* **1993**, *12*, 2079. (r) Fuchita, Y.; Akiyama, M.; Arimoto, Y.; Matsumoto, N.; Okawa, H. *Inorg. Chim. Acta* **1993**, *205*, 185. (s) Fuchita, Y.; Taga, M.; Kawakami, M.; Kawachi, F. *Bull. Chem. Soc. Jpn.* **1993**, *66*, 1294. (t) Fuchita, Y.; Harada, Y. *Inorg. Chim. Acta* **1993**, *208*, 43. (u) Fuchita, Y.; Takeda, Y.; Taga, M. *Inorg. Chim. Acta* **1994**, *216*, 253. (v) Fuchita, Y.; Tsuchiya, H.; Miyafuji, A. *Inorg. Chim. Acta* **1995**, *233*, 91. (w) Fuchita, Y.; Takahashi, K.; Kanehisa, N.; Shinkimoto, K.; Kai, Y.; Kasai, N. *Polyhedron* **1996**, *15*, 2777, and references therein. (x) Fuchita, Y.; Ieda, H.; Tsunemune, Y.; Nagaoka, J.; Kawanano, H. *J. Chem. Soc., Dalton Trans.* **1998**, 791.

(37) Gretz, E.; Oliver, T. F.; Sen, A. *J. Am. Chem. Soc.* **1987**, *109*, 8109.

(38) Vargaftik, M. N.; Stolarov, I. P.; Moiseev, I. I. *J. Chem. Soc., Chem. Commun.* **1990**, 1049.

(39) Kao, L.-C.; Hutson, A. C.; Sen, A. *J. Am. Chem. Soc.* **1991**, *113*, 700.

(40) Sen, A.; Lin, M. *J. Chem. Soc., Chem. Commun.* **1992**, 508.

(41) Horvath, I. T.; Cook, R. A.; Millar, J. M.; Kiss, G. *Organometallics* **1993**, *12*, 8.

(42) Luinstra, G. A.; Labinger, J. A.; Bercaw, J. E. *J. Am. Chem. Soc.* **1993**, *115*, 3004.

(43) (a) Schaller, C. P.; Cummines, C. C.; Wolczanski, P. T. *J. Am. Chem. Soc.* **1996**, *118*, 591. (b) Schafer, D. F., II; Wolczanski, P. T. *J. Am. Chem. Soc.* **1998**, *120*, 4881. (c) Schaller, C. P.; Wolczanski, P. T. *Inorg. Chem.* **1993**, *32*, 131.

(44) Jonas, R. T.; Stack, T. D. P. *J. Am. Chem. Soc.* **1997**, *119*, 8566.

(45) Brown, S. N.; Myers, A. W.; Fulton, J. R.; Mayer, J. M. *Organometallics* **1998**, *17*, 3364.

(46) Periana, R. A.; Taube, D. J.; Gamble, S.; Taube, H.; Satoh, T.; Fujii, H. *Science* **1998**, *280*, 560.

(47) Peters, R. G.; White, S.; Roddick, D. M. *Organometallics* **1998**, *17*, 4493, and references therein.

(48) Vicente, J.; Chicote, M. T.; Lozano, M. I.; Huertas, S. *Organometallics* **1999**, *18*, 753.

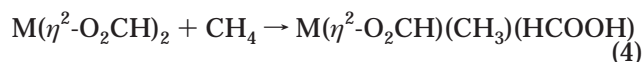
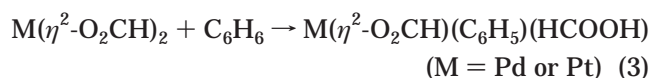
(49) (a) Yoshizawa, K.; Ohta, T.; Yamabe, T.; Hoffmann, R. *J. Am. Chem. Soc.* **1997**, *119*, 12311. (b) Yoshizawa, K.; Shiota, Y.; Yamabe, T. *J. Am. Chem. Soc.* **1998**, *120*, 564. (c) Yoshizawa, K.; Shiota, Y.; Yamabe, T. *J. Am. Chem. Soc.* **1998**, *121*, 147.

(50) Mylvaganam, K.; Bacskay, G. B.; Hush, N. S. *J. Am. Chem. Soc.* **1999**, *121*, 4633.

tion has been presented on the geometry and electronic structure of the transition state and the electronic process and characteristic features of this reaction.

The above-mentioned issues are expected to be investigated successfully with theoretical methods. However, theoretical works of heterolytic C–H bond activation have been limited, as mentioned above.^{49–52} For instance, Yoshizawa and his collaborators theoretically investigated C–H bond activations of methane and benzene by MnO^+ , FeO^+ , and CoO^+ , to afford methanol and phenol.^{49b,c} Also, Hush et al. theoretically investigated Pt(II)-catalyzed C–H bond activation of methane followed by conversion to methanol, while the transition state and the activation energy were not reported.⁵⁰ Siegbahn et al.⁵¹ and Yoshizawa et al.^{49a} reported theoretical studies of the C–H bond activation of methane by biological enzymes. Dedieu and his collaborators theoretically and experimentally investigated base-assisted H–H bond activation and ligand-assisted O–H bond activation, which are similar to heterolytic C–H bond activation.⁵²

In this work, we theoretically investigated the C–H bond activations of benzene and methane by a Pd(II) complex (eqs 3 and 4) with DFT, MP4(SDQ), and



CCSD(T) methods. We adopted here $\text{Pd}(\eta^2\text{-O}_2\text{CH})_2$ as a model of $\text{Pd}(\eta^2\text{-O}_2\text{CMe})_2$, which was experimentally used in the Pd(II)-catalyzed coupling reaction of benzene with alkene.³¹ We also investigated the homolytic C–H bond activations of benzene and methane by Pd(0) and Pt(0) complexes, $\text{M}(\text{PH}_3)_2$ (eqs 5 and 6), and the heterolytic



C–H bond activations of benzene and methane by $\text{Pt}(\eta^2\text{-O}_2\text{CH})_2$, in an attempt to compare the C–H bond activation between M(II) and M(0) complexes and between Pt and Pd. $\text{M}(\text{PH}_3)_2$ was adopted in this work since the σ -bond activation by $\text{M}(\text{PH}_3)_2$ has been theoretically investigated previously,^{23,24d,27} and since Pd(0) complexes with phosphine were several times used as a catalyst (see ref 15 for instance). Our main purpose of this work is to clarify the transition state structure, electronic process, and characteristic features of the heterolytic C–H bond activation.

Computational Details

Geometries of reactants, intermediates, transition states, and products were optimized with the DFT method using the B3LYP functional.^{53,54} Transition state structures were determined by calculating the Hessian matrix. Vibrational frequen-

cies were calculated for some of them. Energy changes were evaluated with ab initio MP4(SDQ), CCSD (coupled cluster with single and double substitutions), and DFT(B3LYP) methods, using the DFT(B3LYP)-optimized geometries. In CCSD calculations, triple excitations were taken into consideration noniteratively.⁵⁵ In all these calculations, core orbitals were excluded from the active space.

Three kinds of basis set systems, BS-I, BS-II, and BS-III, were used in this work. BS-I was employed in the geometry optimization. BS-II and BS-III were used to evaluate energy changes. In BS-I, core electrons of Pd (up to 3d), Pt (up to 4f electrons), and P (up to 2p) were replaced with the effective core potentials (ECPs),^{56,57} and (311/311/31), (311/311/111), and (21/21/1) basis sets were used for valence electrons of Pd, Pt, and P,^{56,57} respectively. MIDI-3⁵⁸ and (31)⁵⁹ sets were employed for C and H, respectively. A p-polarization function ($\zeta = 1.0$) was added to an active H atom, where the H atom of the C–H bond that is broken in the reaction is called here the active H atom. A (421/211) set was used for O of formate, where a p-diffuse function ($\zeta = 0.059$)⁵⁹ was added.

In BS-II, more flexible (541/541/211) and (541/541/111)⁵⁶ sets were used for valence electrons of Pd and Pt, respectively, with the same ECPs as those in BS-I. For P, the same basis set and ECPs as those in BS-I were employed.⁵⁶ A (721/41/1) basis set⁵⁹ was used for C of phenyl and methyl groups. A (31/1)⁵⁹ set was employed for all H atoms except for H of PH_3 and formate, for which a (31) set was used. For C and O of formate, (721/411) basis sets were used, where a p-diffuse function was added to C ($\zeta = 0.034$) and O ($\zeta = 0.059$).⁵⁹

In BS-III, the p-diffuse function was removed from C and O of formate, and the p-polarization function was removed from the H atom of the phenyl group, while the same basis sets and the same ECPs as those of BS-II were used for the other atoms. This basis set system was used for CCSD(T) calculations of the C–H bond activation of benzene by $\text{M}(\eta^2\text{-O}_2\text{CH})_2$ since this reaction system is too large to perform the CCSD(T)/BS-II calculation. Gaussian 98⁶⁰ programs was used in this work.

Results and Discussion

Geometry Changes in the C–H Bond Activations of Benzene and Methane by an M(II) Complex, $\text{M}(\eta^2\text{-O}_2\text{CH})_2$ (M = Pd or Pt). The C–H bond activation reaction of benzene by $\text{M}(\eta^2\text{-O}_2\text{CH})_2$ proceeds through a precursor complex (**PCn**), a transition state (**TSna**) leading to an intermediate (**In**), and a transition state (**TSnb**) leading to a product (**Pn**), as shown in Figure 1, where **n** is 1 for M = Pd and 2 for Pt. Geometry changes of the Pt reaction system are omitted here since they are similar to those of the Pd system (see Support-

(55) Pople, J. A.; Head-Gordon, M.; Raghavachari, K. *J. Chem. Phys.* **1987**, *87*, 5968.

(56) Hay, P. J.; Wadt, W. R. *J. Chem. Phys.* **1985**, *82*, 299.

(57) Wadt, W. R.; Hay, P. J. *J. Chem. Phys.* **1985**, *82*, 284.

(58) Huzinaga, S.; Andzelm, J.; Klobukowski, M.; Radzio-Andzelm, E.; Sakai, Y.; Tatewaki, H. *Gaussian Basis Sets for Molecular Calculations*; Elsevier: Amsterdam, 1984.

(59) Dunning, T. H.; Hay, P. J. In *Methods of Electronic Structure Theory*; Schaeffer, H. F., Ed.; Plenum: New York, 1977; Vol. 4, p 1.

(60) Frisch, M. J.; Trucks, G. W.; Schlegel, H. B.; Scuseria, G. E.; Robb, M. A.; Cheeseman, J. R.; Zakrzewski, V. G.; Montgomery, J. A.; Stratmann, R. E.; Burant, J. C.; Dapprich, S.; Millam, J. M.; Daniels, A. D.; Kudin, K. N.; Strain, M. C.; Farkas, O.; Tomasi, J.; Barone, V.; Cossi, M.; Cammi, R.; Mennucci, B.; Pomelli, C.; Adamo, C.; Clifford, S.; Ochterski, J.; Petersson, G. A.; Ayala, P. Y.; Cui, Q.; Morokuma, K.; Malick, D. K.; Rabuck, A. D.; Raghavachari, K.; Foresman, J. B.; Cioslowski, J.; Ortiz, J. V.; Stefanov, B. B.; Liu, G.; Liashenko, A.; Piskorz, P.; Komaromi, I.; Gomperts, R.; Martin, R. L.; Fox, D. J.; Keith, T.; Al-Laham, M. A.; Peng, C. Y.; Nanayakkara, A.; Gonzalez, C.; Challacombe, M.; Gill, P. M. W.; Johnson, B. G.; Chen, W.; Wong, M. W.; Andres, J. L.; Gonzalez, C.; Head-Gordon, M.; Replogle, E. S.; and Pople, J. A. *Gaussian 98*, Revision A.6; Gaussian, Inc.: Pittsburgh, PA, 1998.

(51) Siegbahn, P. E. M.; Carlbtree, R. H. *J. Am. Chem. Soc.* **1997**, *119*, 3103.

(52) (a) Dedieu, A.; Hutschka, F. *J. Chem. Soc., Dalton Trans.* **1997**, 1899. (b) Hutschka, F.; Dedieu, A.; Eichberger, M.; Fornika, R.; Leitner, W. *J. Am. Chem. Soc.* **1997**, *119*, 4432.

(53) (a) Becke, A. D. *Phys. Rev.* **1988**, *A38*, 3098. (b) Becke, A. D. *J. Chem. Phys.* **1993**, *98*, 5648.

(54) Lee, C.; Yang, W.; Parr, R. G. *Phys. Rev.* **1988**, *B37*, 785.

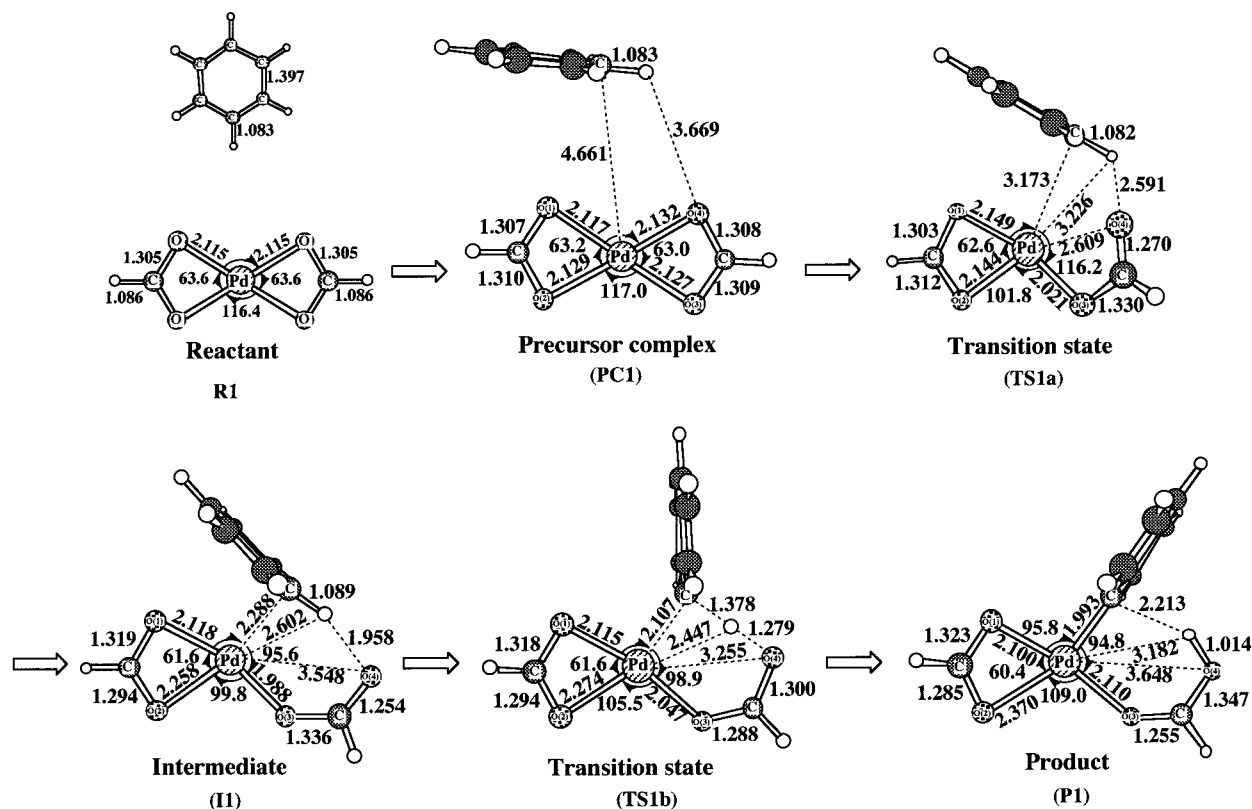


Figure 1. Geometry changes in the C–H bond activation of benzene by $\text{Pd}(\eta^2\text{-O}_2\text{CH})_2$. Bond lengths are in angstroms and bond angles are in degrees.

ing Information). In **PCn**, the M–C distance is 4.66 Å for M = Pd and 4.45 Å for M = Pt, and the O(4)–H distance is about 3.670 Å in both systems. These very long distances clearly indicate a weak interaction between benzene and the $\text{M}(\eta^2\text{-O}_2\text{CH})_2$ moiety. Thus, **PCn** is characterized to be a van der Waals complex, which will be discussed below in more detail. In **TSna**, the M–C and O(4)–H distances become shorter than those of **PCn**, while the M–O(4) distance lengthens by 0.48 Å for M = Pd and 0.51 Å for M = Pt. These features show that benzene is approaching M with replacing one of the O atoms of formate. In **In**, the O(4) atom is very far from Pd and Pt, indicating that only one O atom of the formate ligand interacts with M via $\eta^1\text{-O}$ coordination. The M–C distance is about 2.29 Å, and the benzene ring is almost perpendicular to the M–C bond. The C–H bond that interacts with M moderately bends back away from Pd by 12° and from Pt by 10°. From these features, **I1** and **I2** are considered not a van der Waals complex but an M(II)–benzene complex.

The transition states, **TS1b** and **TS2b**, exhibit only one imaginary frequency: 967 $i\text{ cm}^{-1}$ for **TS1b** and 585 $i\text{ cm}^{-1}$ for **TS2b**. The C–H bond that is broken in the reaction significantly lengthens by 0.289 and 0.223 Å in **TS1b** and **TS2b**, respectively, and the M–C distance of **TS1b** and **TS2b** is only 0.1 Å longer than that of the product, while the O–H distance is considerably longer than that of the product by 0.27 Å in M = Pd and 0.36 Å in M = Pt. These geometrical features suggest that the C–H bond breaking and the O–H bond formation are underway in the transition state, while the M–C bond is nearly formed. It should be noted here that **TS1b** and **TS2b** take a six-centered structure, which will be discussed below.

In **P1**, the calculated Pd–C bond distance (1.993 Å) is slightly shorter than the experimental bond distance (2.092 Å) observed in $[\text{Pd}_3(\text{C}_6\text{H}_3\text{Me}_2)_2(\mu\text{-O}_2\text{CMe})_4\{\text{S}(\text{CH}_2\text{CHMe}_2)_2\}_2]$.³⁶ Since a comparison between mononuclear and trinuclear complexes seems difficult, we also optimized $[\text{Pd}_2(\text{C}_6\text{H}_5)(\eta^2\text{-O}_2\text{CH})(\mu^2\text{-O}_2\text{CH})_2(\text{SH}_2)]$. This is considered a more realistic model of $[\text{Pd}_3(\text{C}_6\text{H}_3\text{Me}_2)_2(\mu\text{-O}_2\text{CMe})_4\{\text{S}(\text{CH}_2\text{CHMe}_2)_2\}_2]$ because $\mu^2\text{-O}_2\text{CH}$ takes a position trans to C_6H_5 like that in the trinuclear complex (remember that the trans-influence is very important for the M–R bonding feature). In the dinuclear complex, the Pd–O distance (2.198 Å) trans to the phenyl group agrees well with the experimental distance (2.167 Å) and the Pd–C distance (2.004 Å) is almost the same as that of **P1**. These results suggest that the Pd– C_6H_5 bonding feature of **P1** is similar to those of the dinuclear and trinuclear complexes and the DFT(B3LYP)/BS-I optimization provides reliable geometry in these complexes.

Interestingly, the H atom of formic acid takes a position perpendicular to the phenyl plane in **P1**. This structure is more stable than the rotation isomer in which formic acid is almost parallel to the phenyl plane by 3.5 kcal/mol (MP4SDQ/BS-II). These results suggest that some stabilization interaction exists between the phenyl plane and the H atom of formic acid. The similar interaction was theoretically reported in benzene–water and benzene–hydrogen chloride complexes.⁶⁴ Actually,

(61) (a) Koga, N.; Obara, S.; Morokuma, K. *J. Am. Chem. Soc.* **1984**, *106*, 4625. (b) Koga, N.; Obara, S.; Kitaura, K.; Morokuma, K. *J. Am. Chem. Soc.* **1985**, *107*, 7109.

(62) (a) Cooper, A. C.; Streib, W. E.; Eisenstein, O.; Caulton, K. G. *J. Am. Chem. Soc.* **1997**, *119*, 9069. (b) Cooper, A. C.; Clot, E.; Huffman, J. C.; Streib, W. E.; Maseras, F.; Eisenstein, O.; Caulton, K. G. *J. Am. Chem. Soc.* **1999**, *121*, 97.

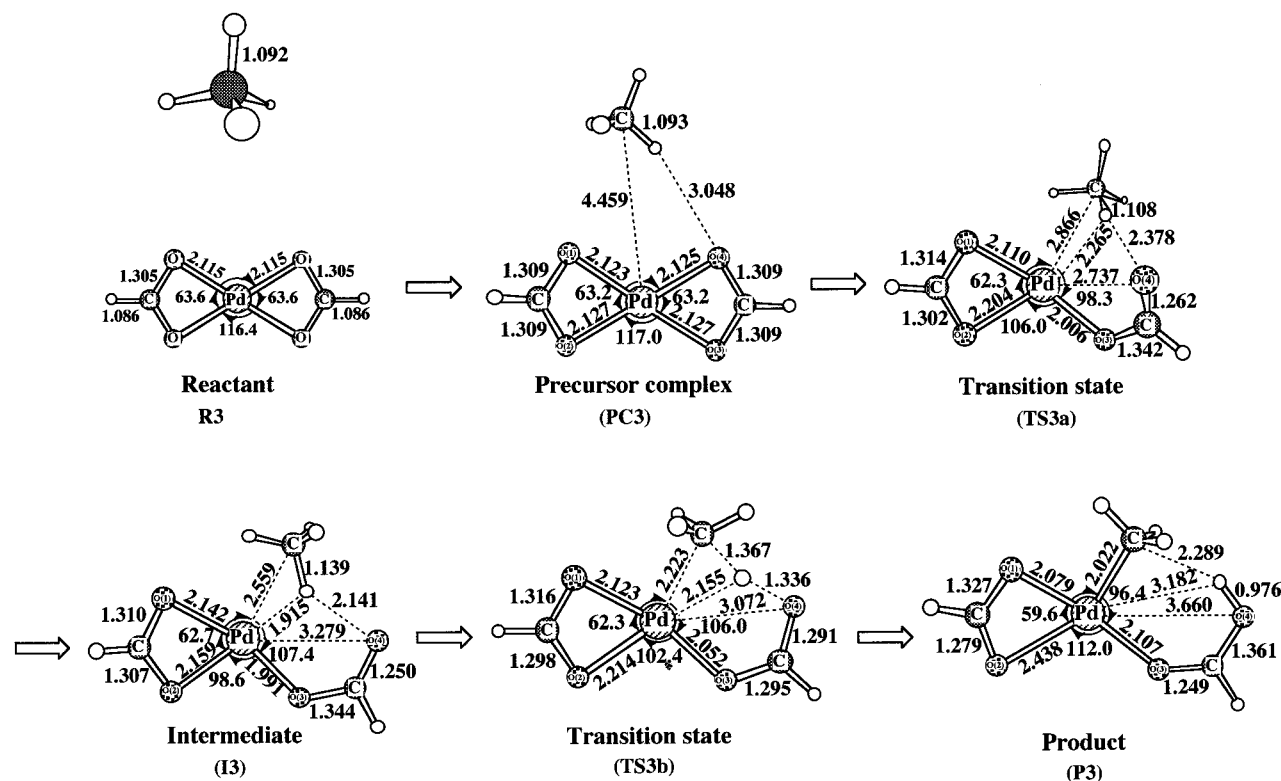


Figure 2. Geometry changes in the C–H bond activation of methane by $\text{Pd}(\eta^2\text{-O}_2\text{CH})_2$. Bond lengths are in angstroms and bond angles are in degrees.

the energy difference of 3.5 kcal/mol between **P1** and the rotation isomer is similar to the binding energies of benzene–water and benzene–hydrogen chloride complexes. The Pd–O(2) distance is much longer than the other Pd–O bond. The same feature is observed in the more realistic complex $[\text{Pd}_2(\text{C}_6\text{H}_5)(\eta^2\text{-O}_2\text{CH})(\mu^2\text{-O}_2\text{CH})_2\text{-(SH}_2)]$ and in the real complex $[\text{Pd}_3(\text{C}_6\text{H}_3\text{Me}_2)_2(\mu\text{-O}_2\text{CMe})_4\{\text{S}(\text{CH}_2\text{CHMe}_2)_2\}_2]$,^{36w} in which the Pd–O bond at a position trans to the phenyl ligand is longer than the other Pd–O bond. This indicates that phenyl and methyl ligands exhibit a stronger trans-influence than HCOOH. The Pd–O(2) distance is 2.110 and 2.107 Å in **P1** and **P2**, respectively. These distances are similar to the M–O distance of **Rn**, which clearly shows that formic acid can coordinate with Pd(II) and Pt(II), like formate.

The C–H bond activation of methane by $\text{Pd}(\eta^2\text{-O}_2\text{CH})_2$ was also investigated, as shown in Figure 2, where geometry changes of the Pt system are omitted too. In **PCn** (**n** = 3 for M = Pd and **n** = 4 for M = Pt), methane is very far from the $\text{M}(\eta^2\text{-O}_2\text{CH})_2$ moiety. In **TS3a** and **TS4a**, methane is approaching M with replacing one O atom of formate, like that in **TS1a** and **TS2a**. Although these features are commonly observed in both C–H bond activations of benzene and methane, interesting differences are observed in **In**: the M–C distance is 2.56 Å for M = Pd and 2.45 Å for M = Pt, which are much longer than those of **I1** and **I2**. The other important difference is found in the C–H and M–H bond distances: the C–H bond considerably lengthens to 1.139

and 1.174 Å for M = Pd and Pt, respectively, being longer than those of **I1** and **I2**. The M–H distance is rather short, 1.915 and 1.798 Å for M = Pd and Pt, respectively, shorter than those of **I1** and **I2**. These geometrical features are similar to those observed in the CH–M agostic interaction systems.^{61–63} Thus, **I3** and **I4** are considered an M(II)–methane complex which is formed by the weak interaction between M(II) and the C–H bonding orbital.

In the second transition state (**TS3b** and **TS4b**), the C–H distance is about 1.37 Å for both Pd and Pt systems. The O–H distance is 1.34 Å for M = Pd and 1.40 Å for M = Pt, and the M–C distance is 2.22 Å for M = Pd and 2.20 Å for M = Pt, which are about 0.2 Å longer than that of the product. From these distances, it is concluded also in the C–H bond activation of methane that the O–H bond formation and the C–H bond breaking are underway in the transition state, while the M–C bond formation is nearly completed. The Pd–C bonds of **P3** and **P4** are longer than those of **P1** and **P2**, respectively. This suggests that the M–CH₃ bond is weaker than the M–C₆H₅ bond, which will be discussed below in more detail. The M–O(2) bond is longer in **P3** and **P4** than in **P1** and **P2**, which suggests that the methyl ligand exhibits stronger trans-influence than the phenyl ligand.

Geometry Changes in the C–H Bond Activations of Benzene and Methane by $\text{M}(\text{PH}_3)_2$. Since the geometry changes of the C–H bond activation of methane by $\text{M}(\text{PH}_3)_2$ were discussed previously,^{27b} we do not repeat the discussion. Here, we will discuss the geometry changes of the C–H bond activation of benzene by $\text{M}(\text{PH}_3)_2$ (M = Pd or Pt). As shown in Figure 3, there are three types of precursor complex, **PCna**, **PCnb**, and

(63) Sakaki, S.; Mizoe, N.; Mushashi, Y.; Sugimoto, M. *Organometallics* **1998**, 17, 2510.

(64) (a) Kim, K. S.; Lee, J. Y.; Choi, H. S.; Kim, J.; Jang, J. H. *Chem. Phys. Lett.* **1997**, 265, 497. (b) Tarakeswar, P.; Lee, S. J.; Lee, J. Y.; Kim, K. S. *J. Chem. Phys.* **1998**, 108, 7217.

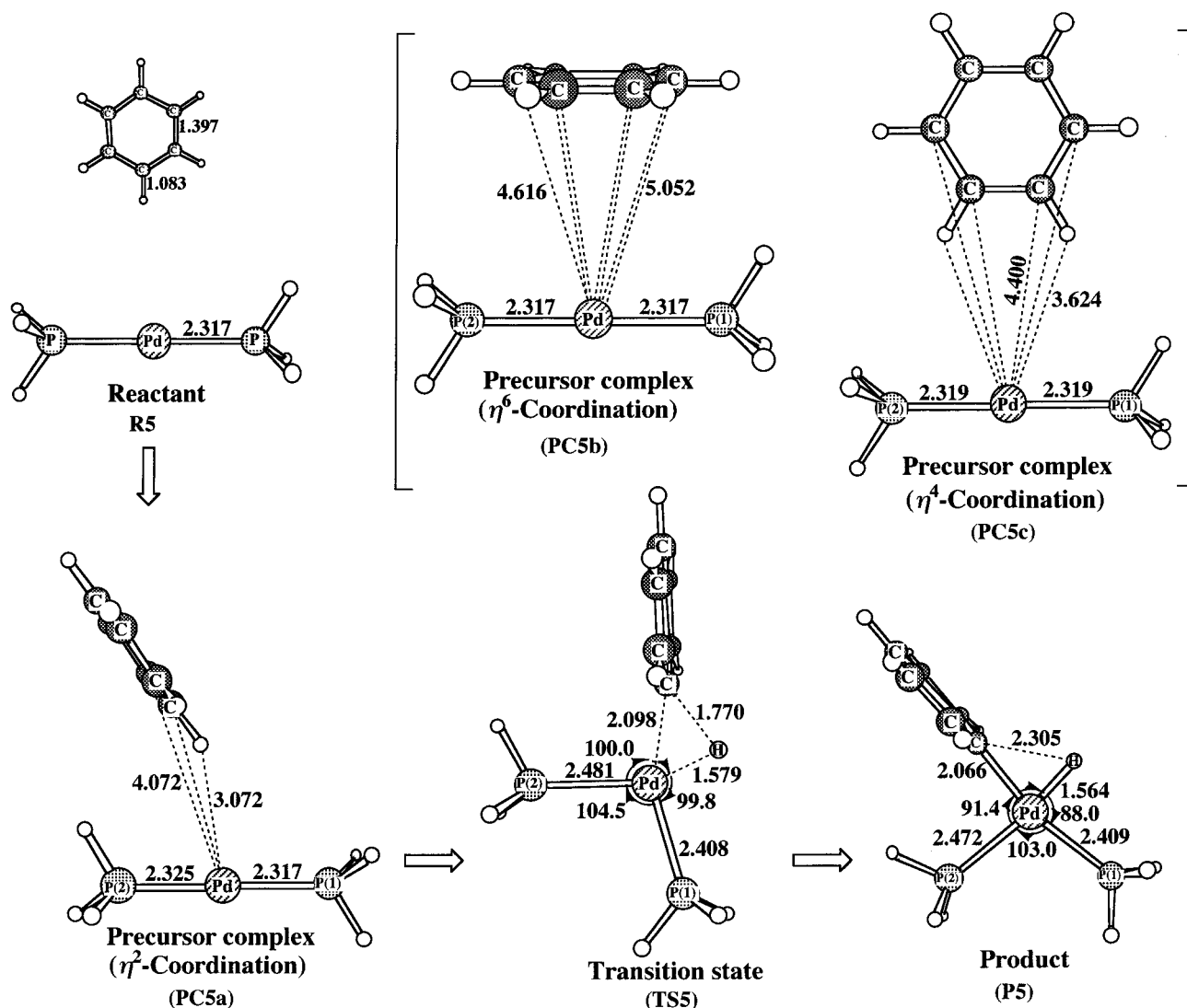


Figure 3. Geometry changes in the C-H bond activation of benzene by $\text{Pd}(\text{PH}_3)_2$. Bond lengths are in angstroms and bond angles are in degrees.

PCnc ($n = 5$ and 6 for Pd and Pt, respectively).⁶⁵ **PCna** is the most stable in them, while the energy difference is small; about 2 kcal/mol in $M = \text{Pd}$ and 4 kcal/mol in $M = \text{Pt}$. In **PCna**, the M-C and M-H distances are very long and both $M(\text{PH}_3)_2$ and benzene moieties little distort. From these features, **PCna** can be characterized to be a van der Waals complex like the precursor complexes observed in the oxidative addition of the C-H bond of methane to $M(\text{PH}_3)_2$.^{27a,66} In **PCna**, benzene is much more distant from M than in **I1** and **I2**. This suggests that M(0) more weakly interacts with benzene than does M(II).

In the transition states **TS5** and **TS6**, the C-H bond that is broken in the reaction is longer than those of **PC5a** and **PC6a** by 0.69 and 0.4 Å, respectively. The C_6H_5 group is changing its direction toward M, and the M-C $_6\text{H}_5$ and M-H distances are slightly longer than those of the products **P5** and **P6** by only 0.032 and 0.015 Å, respectively, in $M = \text{Pd}$ and 0.093 and 0.072 Å,

respectively, in $M = \text{Pt}$. The P(2)-M-P(1) angles of **TS5** and **TS6** are almost the same as those of **P5** and **P6**, respectively. All these features indicate that these TS's are product-like. In **P5** and **P6**, the M-P(2) bond at a position trans to H(hydride) is longer than the M-P(1) bond at a position trans to the C_6H_5 ligand. The similar geometrical features were observed in *cis*-MH(CH_3)-(PH_3)₂.^{27b} These results indicate that trans-influence increases in the order $\text{CH}_3 < \text{C}_6\text{H}_5 < \text{H}$ (hydride). This increasing order is a little bit different from the order observed in $M(\eta^2\text{-O}_2\text{CH})(\text{CH}_3)(\text{HCOOH})$ (vide supra). This difference would arise from the coordinate bond nature of $M-(\eta^2\text{-O}_2\text{CH})$ and $M\text{-PH}_3$.⁶⁷

Energy Changes in the C-H Bond Activations of Benzene and Methane by $M(\eta^2\text{-O}_2\text{CH})_2$ and $M(\text{PH}_3)_2$. A binding energy (BE), an activation energy (E_a), and a reaction energy (ΔE) were calculated with

(65) We tried to optimize the η^4 -coordination structure in which benzene coordinates with Pd(0) through four C atoms. However, the geometry optimization led to **PC3c**.

(66) Sakaki, S.; Ogawa, M.; Musashi, Y.; Arai, T. *Inorg. Chem.* **1994**, *33*, 1660.

(67) The coordinate bond of $\eta^2\text{-O}_2\text{CH}$ does not involve a π -back-donation interaction, while the coordinate bond of PH_3 would involve a π -back-donation interaction. Its π -interaction is weakened by the π -back-donation between Pd and the C_6H_5 group. Thus, the trans-influence to Pd- PH_3 increases in the order $\text{CH}_3 < \text{C}_6\text{H}_5 < \text{H}$ (hydride). In the Pd- $(\eta^2\text{-O}_2\text{CH})$ bond, only the σ -interaction is important. As a result, the trans-influence increases in the order $\text{C}_6\text{H}_5 < \text{CH}_3 < \text{H}$ (hydride).

Table 1. Basis Set Effects on the Binding Energy (BE), Activation Energy (E_a), and Reaction Energy (ΔE) (kcal/mol) in the C–H Bond Activation of Benzene by $M(\eta^2\text{-O}_2\text{CH})_2$ (M = Pd or Pt)

	Pd					Pt				
	DFT (B3LYP)			MP4(SDQ)		DFT (B3LYP)			MP4(SDQ)	
	BS-I	BS-II	BS-III	BS-II	BS-III	BS-I	BS-II	BS-III	BS-II	BS-III
BE ^a	−1.7	−0.03	−0.3	−2.3	−0.7	−1.5	−0.2	−0.4	−3.7	−1.9
$E_a(1)^b$	5.1	5.4	5.2	3.7	2.8	9.1	9.4	9.4	6.5	5.7
$E_a(2)^c$	14.1	10.5	9.9	16.1	15.7	12.3	11.4	10.7	21.2	20.9
ΔE^d	−4.6	−12.0	−12.4	−16.5	−17.2	−11.5	−19.3	−19.3	−25.8	−26.1

^a BE = $E_t(\text{precursor complex}) - E_t(\text{sum of reactants})$. ^b $E_a(1) = E_t(\text{TS1a}) - E_t(\text{precursor complex})$. ^c $E_a(2) = E_t(\text{TS1b}) - E_t(\text{immediate})$. ^d $\Delta E = E_t(\text{product}) - E_t(\text{sum of reactants})$.

Table 2. Binding Energy (BE), Activation Energy (E_a), and Reaction Energy (ΔE) of the C–H Bond Activations of Benzene and Methane by $M(\eta^2\text{-O}_2\text{CH})_2$ and $M(\text{PH}_3)_2$ (M = Pd or Pt) (kcal/mol unit)

method	Pd($\eta^2\text{-O}_2\text{CH})_2 + \text{CH}_4^a$			Pd($\eta^2\text{-O}_2\text{CH})_2 + \text{C}_6\text{H}_6^b$			Pd(PH ₃) ₂ + CH ₄ ^a			Pd(PH ₃) ₂ + C ₆ H ₆ ^a		
	BE ^c	E_a^d	ΔE^e	BE ^c	E_a^f	ΔE^g	BE ^c	E_a^g	ΔE^h	BE ^c	E_a^g	ΔE^h
MP2	−1.3	17.5	−12.8	−0.9	11.5	−24.0	−0.7	31.5	28.3	−4.0	20.2	16.6
MP3	−1.2	19.8	−12.8	−0.4	15.8	−20.4	−0.6	37.6	31.2	−3.4	28.5	21.7
MP4DQ	−1.2	21.1	−12.0	−0.4	16.3	−19.5	−0.6	35.6	31.3	−3.5	27.0	22.2
MP4(SDQ)	−1.3	21.5	−8.3	−0.7	15.7	−17.2	−0.7	34.7	31.5	−3.8	26.5	22.1
CCSD(T)	−1.5	20.5	−6.1	−1.0	14.1	−17.5	−0.7	34.4	28.8	−4.0	24.1	17.2
DFT(B3LYP)	−0.6	13.9	−4.9	−0.3	9.9	−12.4	−0.1	35.1	31.0	−2.0	28.9	24.5
method	Pd($\eta^2\text{-O}_2\text{CH})_2 + \text{CH}_4^a$			Pd($\eta^2\text{-O}_2\text{CH})_2 + \text{C}_6\text{H}_6^b$			Pd(PH ₃) ₂ + CH ₄ ^a			Pd(PH ₃) ₂ + CH ₄ ^a		
	BE ^c	E_a^d	ΔE^e	BE ^c	E_a^f	ΔE^g	BE ^c	E_a^g	ΔE^h	BE ^c	E_a^g	ΔE^h
MP4(SDQ)	−2.6	17.3	−13.3	−1.9	20.9	−24.1	−0.7	28.2	7.0	−5.3	17.1	−3.9
CCSD(T)	−3.0	17.7	−12.6	−2.5	20.0	−24.7	−0.7	28.5	5.2	−5.4	16.2	−7.2
DFT(B3LYP)	−0.8	11.3	−10.5	−0.4	10.7	−19.3	−0.1	32.1	12.0	−3.1	24.0	4.9

^a BS-II was used. ^b BS-III was used. ^c BE = $E_t(\text{precursor complex}) - E_t(\text{sum of reactants})$. ^d $E_a = E_t(\text{TSnb}) - E_t(\text{PCn})$. ^e $\Delta E = E_t(\text{product}) - E_t(\text{sum of reactants})$. ^f $E_a = E_t(\text{TSnb}) - E_t(\text{intermediate})$. ^g $E_a = E_t(\text{TS}) - E_t(\text{precursor complex})$.

MP2–MP4(SDQ), CCSD(T), and DFT(B3LYP) methods, where BE is the energy difference between **PCn** and the sum of reactants, $E_a(1)$ is the energy difference between **TSna** and **PCn**, $E_a(2)$ is the energy difference between **TSnb** and **In**, and ΔE is the energy difference between the final product and the sum of reactants. A negative ΔE value represents that the reaction is exothermic. First, a comparison between BS-II and BS-III was made in the C–H bond activation of benzene by $M(\eta^2\text{-O}_2\text{CH})_2$, to examine effects of the p-diffuse functions of C and O of formate and the effects of the p-polarization function of H in the phenyl group. In MP4(SDQ) calculation, the energy difference between BS-II and BS-III is 1.6 kcal/mol for BE, 0.9 kcal/mol for $E_a(1)$, 0.4 kcal/mol for $E_a(2)$, and 0.7 kcal/mol for ΔE , when M = Pd. In the DFT(B3LYP) calculation, the energy difference is 0.2 and 0.6 kcal/mol for $E_a(1)$ and $E_a(2)$, respectively, and 0.4 kcal/mol for ΔE , when M = Pd. The differences of the Pt reaction system are as small as the above-mentioned differences of the Pd reaction system. Since these differences between BS-II and BS-III are not significant, the quality of basis set seems almost saturated upon going to BS-II from BS-III. This means that BS-II and BS-III are useful for investigation of this type of C–H bond activation. Also, E_a and ΔE values from DFT/BS-I calculations are shown in Table 1. These values differ greatly from those of DFT/BS-II and DFT/BS-III calculations, indicating the well-known fact that the d-polarization function is necessary to estimate reliable energy changes. Here, we mainly used BS-II.

It should also be noted that $E_a(1)$, $E_a(2)$, and ΔE values are significantly different between MP4(SDQ) and DFT methods. To investigate whether MP4(SDQ) or DFT(B3LYP) is more reliable, we carried out the CCSD(T) calculation. Since the reaction system of C–H

bond activation of benzene by $M(\eta^2\text{-O}_2\text{CH})_2$ is too large to perform the CCSD(T)/BS-II calculation, we adopted BS-III only for this system. As shown in Table 2, E_a and ΔE values moderately fluctuate upon going from MP2 to MP4(DQ) but change little upon going from MP4(SDQ) to CCSD(T) except for the C–H bond activation of benzene by $M(\text{PH}_3)_2$, in which the CCSD(T) method provides somewhat smaller E_a and ΔE values than MP4(SDQ) and DFT(B3LYP) methods. However, the DFT(B3LYP) method gives much smaller E_a and ΔE values in the C–H bond activations of benzene and methane by $M(\eta^2\text{-O}_2\text{CH})_2$ and larger E_a and ΔE values in the C–H bond activation of benzene by $M(\text{PH}_3)_2$ than MP4(SDQ) and CCSD(T) methods. From these results, it is clearly concluded that the DFT(B3LYP) method significantly underestimates the E_a and ΔE values in the C–H bond activation by $M(\eta^2\text{-O}_2\text{CH})_2$ and that the MP4(SDQ) method seems more reliable than the DFT(B3LYP) method in these C–H bond activation reactions. We present our discussion based on the MP4(SDQ)/BS-II calculation.

Energy changes in all the C–H bond activations examined here are displayed in Figure 4. The BE values are very small in all the reaction systems, which is consistent with our understanding from the geometrical features that benzene and methane weakly interact with $M(\eta^2\text{-O}_2\text{CH})_2$ and $M(\text{PH}_3)_2$ moieties in **PCn** (**n** = 1–4) and **PCna** (**n** = 5, 6), and these precursor complexes are considered van der Waals complexes.

In the C–H bond activation of benzene by $M(\eta^2\text{-O}_2\text{CH})_2$, the $E_a(1)$ value for the first transition state is 3.8 kcal/mol in M = Pd and 6.6 kcal/mol in M = Pt, and the $E_a(2)$ value for the second transition state is 16.1 kcal/mol in M = Pd and 21.3 kcal/mol in M = Pt. The intermediate **I1** is 9.8 kcal/mol more stable than the reactant in the Pd reaction system, whereas **I2** is

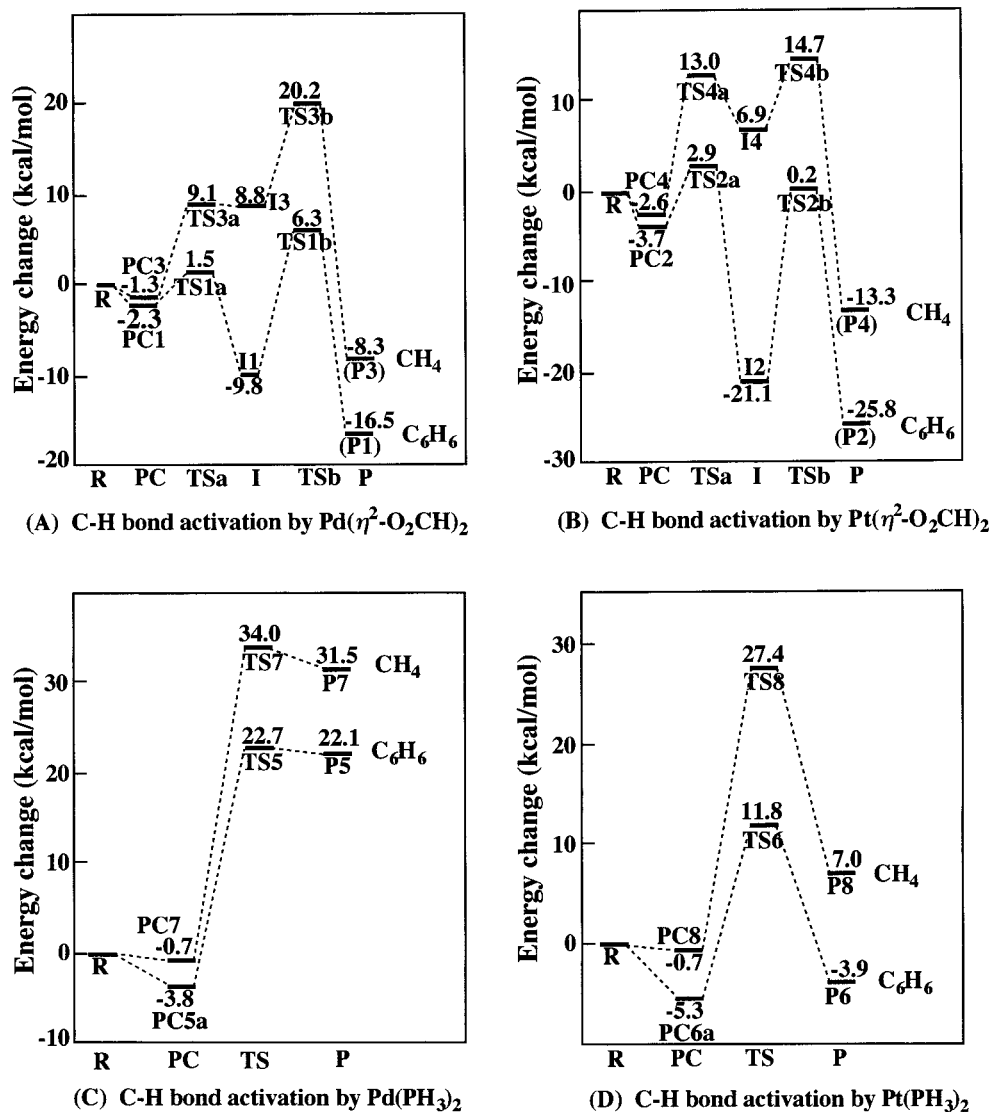


Figure 4. Energy changes by the C–H bond activations of benzene and methane by $\text{Pd}(\eta^2\text{-O}_2\text{CH})_2$ (A) and $\text{Pd}(\text{PH}_3)_2$ (B). Energies are given in kcal/mol (relative to reactants; MP4SDQ/BS-II). **R**, **PC**, **TSa**, **I**, **TSb**, and **P** represent the reactant, the precursor complex, the first transition state, the intermediate, the second transition state, and the product, respectively (see Figures 1–3 for details).

considerably more stable than the reactant by 21.1 kcal/mol in the Pt reaction system. This obviously implies that benzene more strongly coordinates with M(II) than does the O(4) atom of formate and that the benzene coordination to Pt(II) is much stronger than that to Pd(II). The product is significantly more stable than the sum of reactants by 16.5 kcal/mol for $M = \text{Pd}$ and 25.8 kcal/mol for $M = \text{Pt}$. In the C–H bond activation of methane by $\text{Pd}(\eta^2\text{-O}_2\text{CH})_2$, the intermediate **I3** is only slightly more stable than **TS3a** by 0.3 kcal/mol and much less stable than the reactant. In the Pt reaction system, the intermediate **I4** is ca. 6 kcal/mol more stable than **TS4a** but still much less stable than the reactant by ca. 7 kcal/mol. The small stabilities of **I3** and **I4** are consistent with their long M–C distances. These results also indicate that methane does not coordinate strongly with M(II), unlike benzene, because methane does not have a good donor orbital but benzene has π orbitals. Because of small stabilities of **I3** and **I4** relative to **TS3a** and **TS4a**, we defined the activation barrier as an energy difference between **TSnb** and **PCn** ($n = 3$ and

4). The estimated activation barrier is 21.5 kcal/mol for $M = \text{Pd}$ and 17.3 kcal/mol for $M = \text{Pt}$.

On the other hand, the C–H bond activations of benzene and methane by $\text{Pd}(\text{PH}_3)_2$ require a significantly large activation barrier, and these reactions are considerably endothermic. The reverse reaction (i.e., C–H reductive elimination) more easily occurs with a much smaller activation barrier than the forward C–H bond activation. The C–H bond activation of benzene by $\text{Pt}(\text{PH}_3)_2$ occurs with a moderate activation barrier of 17.1 kcal/mol and a small exothermicity of 3.9 kcal/mol, while the C–H bond activation of methane by $\text{Pt}(\text{PH}_3)_2$ requires a large activation barrier (28.4 kcal/mol) and the reaction is endothermic ($\Delta E = 7.0$ kcal/mol).

From the above results, the following conclusions are presented: (1) The C–H bond activation of benzene by $\text{Pd}(\eta^2\text{-O}_2\text{CH})_2$ proceeds with a lower activation barrier than that by $\text{Pt}(\eta^2\text{-O}_2\text{CH})_2$, whereas the former reaction is much less exothermic than the latter. This is because benzene strongly coordinates with Pt(II) to stabilize the

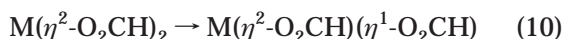
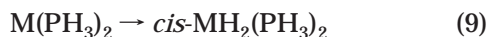
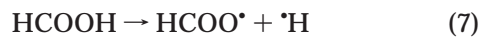
Table 3. Bond Energies (kcal/mol)^a

system	bond energy	MP4(SDQ)	CCSD	CCSD(T)	B3LYP
HCOOH	<i>E</i> (O–H)	114.4	108.9	107.0	113.1
Pd(η^2 -O ₂ CH) ₂	<i>E</i> (Pd–O)	23.0	21.8	23.2	21.9
Pt(η^2 -O ₂ CH) ₂	<i>E</i> (Pt–O)	24.5	24.0	24.8	25.9
<i>cis</i> -Pd(H) ₂ (PH ₃) ₂	<i>E</i> (Pd–H)	48.5	49.5	49.5	52.8
<i>cis</i> -Pt(H) ₂ (PH ₃) ₂	<i>E</i> (Pt–H)	60.2	61.0	60.8	61.8
CH ₄	<i>E</i> (C–H)	108.6	108.4	109.0	112.5
C ₆ H ₆	<i>E</i> (C–H)	129.0	118.8	119.0	119.7
<i>cis</i> -Pd(H)(CH ₃)(PH ₃) ₂	<i>E</i> (Pd–CH ₃)	28.7	28.5	30.7	28.8
<i>cis</i> -Pt(H)(CH ₃)(PH ₃) ₂	<i>E</i> (Pt–CH ₃)	41.0	41.2	42.9	38.6
<i>cis</i> -Pd(H)(C ₆ H ₅)(PH ₃) ₂	<i>E</i> (Pd–C ₆ H ₅)	57.6	48.3	51.4	41.0
<i>cis</i> -Pt(H)(C ₆ H ₅)(PH ₃) ₂	<i>E</i> (Pt–C ₆ H ₅)	73.3	60.8	63.4	51.2

^a BS-II was used.

intermediate (**12**) too much. (2) The C–H bond activation of methane by Pt(η^2 -O₂CH)₂ more easily occurs than that by Pd(η^2 -O₂CH)₂. (3) Although the C–H bond activation of methane by Pd(η^2 -O₂CH)₂ requires a considerably large *E_a* value of about 22 kcal/mol, this reaction might occur because the reverse reaction is more difficult than the forward C–H bond activation. And, (4) the C–H bond activations of methane and benzene by Pd(PH₃)₂ are much more difficult than those by Pd(η^2 -O₂CH)₂ and Pt(PH₃)₂.

Comparison of the Reaction Energy between M(η^2 -O₂CH)₂ and M(PH₃)₂. One of the significant differences between M(η^2 -O₂CH)₂ and M(PH₃)₂ is that the C–H bond activation by M(η^2 -O₂CH)₂ is very exothermic but the C–H bond activation by M(PH₃)₂ is much more endothermic (or much less exothermic). Because of the large endothermicity, the C–H bond activation by Pd(PH₃)₂ is difficult, but the reverse reaction easily occurs. However, because of the large exothermicity, the C–H bond activation by Pd(η^2 -O₂CH)₂ easily occurs, but the reverse reaction is difficult. Thus, it is important to investigate the reason that the C–H bond activation by Pd(η^2 -O₂CH)₂ is very exothermic but the C–H bond activation by Pd(PH₃)₂ is endothermic. In the C–H bond activation of benzene by M(η^2 -O₂CH)₂, the C–H bond of benzene and the M–O bond of M(η^2 -O₂CH)₂ are broken, while the M–C₆H₅ and O–H bonds are formed. In the C–H bond activation of benzene by M(PH₃)₂, the C–H bond of benzene is broken and the M–C₆H₅ and M–H bonds are formed. Thus, the reactivity difference between M(η^2 -O₂CH)₂ and M(PH₃)₂ would arise from the difference between the O–H, M–O, and M–H bond strengths. We estimated the O–H and M–H bond energies by considering eqs 7, 8, and 9. The M–O bond energy is defined here as an energy change by eq 10, where the geometry of M(η^2 -O₂CH)(η^1 -OCOH) was optimized with the B3LYP/BS-I method.



As shown in Table 3, the O–H bond is much stronger than the M–O bond by 83.8–85.5 kcal/mol. This difference is much greater than the M–H bond energy. These results clearly indicate that the formation of the strong O–H bond leads to the significantly large exothermicity

of the C–H bond activation by M(η^2 -O₂CH)₂. In other words, the C–H bond activation by M(η^2 -O₂CH)₂ is assisted by the formation of the strong O–H bond, and the coexisting ligand that reacts with the active H atom plays an important role in the heterolytic C–H bond activation. The present result provides a theoretical support to the experimental proposal that the role of acetate ligand is to facilitate the proton abstraction from benzene in the C–H bond activation by Pd(η^2 -O₂CH)₂.^{1d}

Comparison of the Reaction Energy between Benzene and Methane. The reactivity difference between benzene and methane is also an important issue to be investigated. To clarify the reasons that the reaction of benzene is more exothermic (or less endothermic) than that of methane, we examined here the C–H, M–C₆H₅, and M–CH₃ bond energies. The C–H bond energies of benzene and methane were estimated by considering the following reactions:



The M–C₆H₅ and M–CH₃ bond energies were estimated through two steps: In the first step, the M–H bond energy was estimated as discussed above, and then the sum of M–H and M–C₆H₅ bond energies and that of M–H and M–CH₃ bond energies were calculated with eqs 13 and 14, respectively. In the second step, the M–C₆H₅ and M–CH₃ bond energies were evaluated by subtracting the M–H bond energy from these sums.



As shown in Table 3, the C–H bond of benzene is stronger than that of methane by 10 kcal/mol, while the M–C₆H₅ bond is stronger than the M–CH₃ bond by 19.7 kcal/mol for M = Pd and 20.5 kcal/mol for M = Pt. Accordingly, the C–H bond activation of benzene is more exothermic (or less endothermic) than the C–H bond activation of methane.

Why is the M–C₆H₅ bond stronger than the M–CH₃ bond? This result can be easily interpreted in terms of simple molecular orbital consideration, as follows: the total electronic stabilization energy ($\Delta\epsilon_t$) from covalent bond formation is represented by eq 15,^{27c}

$$\Delta\epsilon_t = \alpha_A - \alpha_B + 2\beta^2/(\alpha_A - \alpha_B) \quad (15)$$

where α_A and α_B represent the d orbital energy of the

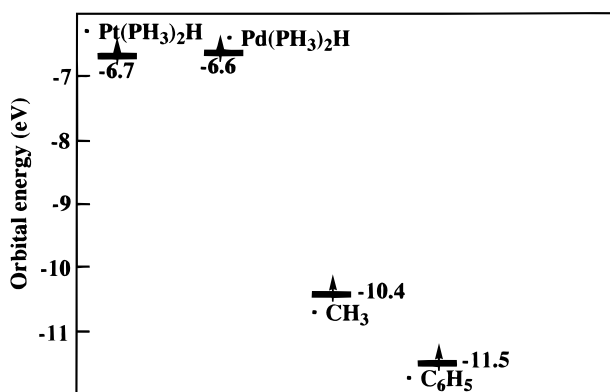


Figure 5. Energy levels of the d_o orbital of $\text{Pd(PH}_3)_2\text{H}$, $\text{Pt(PH}_3)_2\text{H}$, sp^3 radical orbital of •CH_3 (A), and sp^2 radical orbital of $\text{•C}_6\text{H}_5$ (B).

metal and either the sp^3 radical orbital energy of •CH_3 or the sp^2 radical orbital energy of $\text{•C}_6\text{H}_5$, respectively, and β is an usual resonance integral. Equation 15 indicates that $\Delta\epsilon_t$ increases with an increase of the $\alpha_A - \alpha_B$ value, when the $\alpha_A - \alpha_B$ value is larger than the $\sqrt{2}|\beta|$ value. As shown in Figure 5, the •CH_3 sp^3 and $\text{•C}_6\text{H}_5$ sp^2 orbitals were calculated to be at -10.4 and -11.5 eV, respectively, and the d_o orbital of $\text{Pt(PH}_3)_2\text{H}$ was calculated to be at -6.7 eV for Pt. Since the energy difference between α_A and α_B is very large, the $\alpha_A - \alpha_B$ value would be larger than the $\sqrt{2}|\beta|$ value. Thus, the $\text{M-C}_6\text{H}_5$ and M-CH_3 bond energies increase with an increase of the $\alpha_A - \alpha_B$ value. As apparently shown in Figure 5, the sp^2 orbital of $\text{•C}_6\text{H}_5$ is at a lower energy than the sp^3 orbital of •CH_3 . This is one of the important reasons that the $\text{M-C}_6\text{H}_5$ bond is stronger than the M-CH_3 bond. In addition, the π -back-donating interaction between $\text{M } d\pi$ and $\text{C}_6\text{H}_5 \pi^*$ orbitals might contribute to the $\text{M-C}_6\text{H}_5$ bond. This is also the other reason of the stronger $\text{M-C}_6\text{H}_5$ bond than the M-CH_3 bond.

Comparison of Reactivity between Pd and Pt.

In the C–H bond activation of benzene, $\text{Pt}(\eta^2\text{-O}_2\text{CH})_2$ needs the larger E_a value than $\text{Pd}(\eta^2\text{-O}_2\text{CH})_2$. This means that $\text{Pd}(\eta^2\text{-O}_2\text{CH})_2$ is more favorable for the C–H bond activation of benzene than the Pt analogue. As clearly shown in Figure 4, the large stability of intermediate, Pt(II)-benzene complex **12**, leads to the large E_a value of the C–H bond activation of benzene by $\text{Pt}(\eta^2\text{-O}_2\text{CH})_2$. On the other hand, the C–H bond activation of methane by $\text{Pt}(\eta^2\text{-O}_2\text{CH})_2$ occurs with a smaller E_a value than that by $\text{Pd}(\eta^2\text{-O}_2\text{CH})_2$. This difference in the E_a value between Pt(II) and Pd(II) complexes is similar to the difference in the ΔE value between them. Thus, it is clearly concluded that $\text{Pt}(\eta^2\text{-O}_2\text{CH})_2$ is more favorable for the C–H bond activation of methane than the Pd analogue because of the larger exothermicity.

These results come from the fact that Pt(II) can form a stronger bonding interaction with benzene, phenyl, and methyl groups. Benzene coordinates with Pt(II) much more strongly than with Pd(II) . As a result, the Pt(II)-benzene complex is too stable and $\text{Pt}(\eta^2\text{-O}_2\text{CH})_2$ needs a larger E_a value than $\text{Pd}(\eta^2\text{-O}_2\text{CH})_2$ in the C–H bond activation of benzene. In the C–H bond activation of methane, methane does not coordinate strongly with Pd(II) and Pt(II) , and therefore, not the stability of the intermediate but the stability of the product becomes a

determining factor of the reactivity. This leads to the larger reactivity of $\text{Pt}(\eta^2\text{-O}_2\text{CH})_2$ than that of the Pd analogue in the C–H activation of methane. The reason the Pt-CH_3 bond is stronger than the Pd-CH_3 bond was previously interpreted in terms of the larger orbital overlaps between Pt and C valence orbitals than those between Pd and C valence orbitals.⁶⁸ The stronger $\text{Pt-C}_6\text{H}_5$ bond than the $\text{Pd-C}_6\text{H}_5$ bond is explained in terms of the same reason. Also, the Pt d orbital contributes more to the π -back-donation from the Pt $d\pi$ to the π^* orbital of the C_6H_5 group than the Pd d orbital, because the former is at a higher energy than the latter. This is the other reason for the stronger $\text{Pt-C}_6\text{H}_5$ bond.

Since a comparison between $\text{Pd(PH}_3)_2$ and $\text{Pt(PH}_3)_2$ has been discussed previously,²⁴ we do not repeat the discussion here.

Population Changes in the C–H Bond Activation by $\text{M}(\eta^2\text{-O}_2\text{CH})_2$ and $\text{M(PH}_3)_2$. Electron distribution changes were inspected with the natural bond orbital (NBO) population analysis.⁶⁹ It should be noted that the electron population of the active H atom significantly decreases in the reaction (see Figure 6), which clearly indicates that the active H atom changes into a proton in the reaction. This result theoretically supports the experimental proposal that proton abstraction by the carboxylate ligand occurs in the reaction.^{1d}

The population changes shown in Figure 6 are reasonably interpreted by considering the geometry changes. In **TSna**, one of the oxygen atoms of η^2 -formate is going to eliminate from M, while benzene and methane do not interact sufficiently with M(II) . As a result, the electron donation from the formate ligand to M(II) weakens, but the electron donation from benzene and methane does not sufficiently occur, which leads to the decrease in the M atomic population at **TSna**. In **In**, the C–H bonds of benzene and methane interact with an empty d_o orbital of M(II) , like the well-known agostic interaction that is formed through the charge-transfer interaction between an occupied C–H bonding orbital and an empty d_o orbital.⁶¹ Also, the π orbital of benzene interacts with the empty d_o orbital of M to form a charge-transfer interaction. Thus, the M atomic population increases and the electron populations of benzene and methane decrease. Upon going from **In** to **Pn**, one of the oxygen atoms of formate approaches the active H atom of benzene and methane, which induces such polarization as $(\text{C}_6\text{H}_5)^\delta- - \text{H}^\delta+$ and $(\text{CH}_3)^\delta- - \text{H}^\delta+$. This polarization significantly decreases the H atomic population and increases electron populations of C_6H_5 and CH_3 groups, to enhance the charge transfer from C_6H_5 and CH_3 groups to Pd and Pt and to cause further increase of the M atomic population. These population changes clearly indicate that this reaction is characterized to be an electrophilic attack of M to benzene and methane, which concomitantly occurs with proton abstraction by the carboxylate ligand. Again, the present results support the experimental suggestion^{1c,31} that the C–H bond activation of benzene by Pd(II) acetate occurs through electrophilic attack of Pd(II) to benzene.

Here, it should be noted that the electron population of the C_6H_5 group increases in the Pt system to a greater

(68) Sakaki, S.; Kai, S.; Sugimoto, M. *Organometallics* **1999**, *18*, 4825.

(69) Reed, A. E.; Curtiss, L. A.; Weinhold, F. *Chem. Rev.* **1988**, *88*, 849, and references therein.

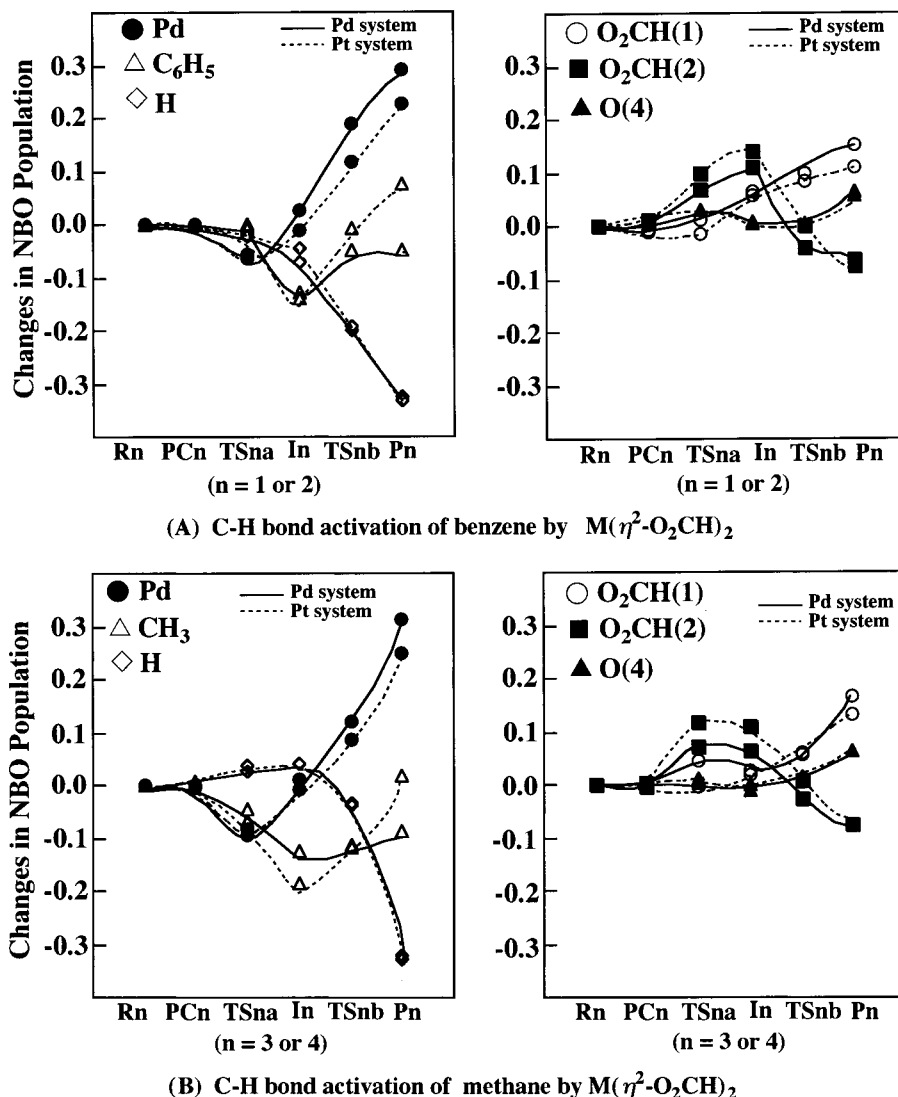


Figure 6. Population changes in the C–H bond activations of benzene (A) and methane (B) by $M(\eta^2\text{-O}_2\text{CH})_2$ and $M(\text{PH}_3)_2$ ($M = \text{Pd}$ or Pt). A positive value represents an increase in population (vice versa). Solid lines represent population change for $M = \text{Pd}$, and dotted lines represent population changes for $M = \text{Pt}$.

extent than that in the Pd system upon going from **In** to **Pn** (see Figure 6A). Consistent with this, the Pd atomic population increases more than does the Pt atomic population. This is because Pd(II) is a stronger electrophile than Pt(II), as mentioned before,²⁴ and the charge transfer from C_6H_5 to Pt(II) occurs less easily than that to Pd(II). The other interesting change is observed in the $\eta^2\text{-O}_2\text{CH}^{(2)}$ ligand that reacts with the active H atom of benzene and methane; its population significantly increases upon going to **In** but then decreases upon going to **Pn** (Figure 6). This is because the $\eta^2\text{-O}_2\text{CH}^{(2)}$ ligand changes to the $\eta^1\text{-O}_2\text{CH}^{(2)}$ ligand in **In** but then changes into formic acid upon going from **In** to **Pn**. The electron population of the other $\eta^2\text{-O}_2\text{CH}^{(1)}$ ligand gradually increases upon going to **Pn** from **Rn**, since more electron-donating C_6H_5 and CH_3 coordinate with M in **Pn** to suppress the electron donation from $\eta^2\text{-O}_2\text{CH}^{(1)}$ to M.

Completely different population changes are observed in the C–H bond activation by $M(\text{PH}_3)_2$. In this C–H bond activation, electron populations of H and R ($R = \text{C}_6\text{H}_5$ or CH_3) increase, while the M atomic population decreases, as shown in Figure 7. These changes are

consistent with our understanding that this C–H bond activation is characterized to be an oxidative addition reaction. Interestingly, the electron population of the C_6H_5 moiety increases to a greater extent than that of the CH_3 moiety in the TS, while the H atomic population similarly increases in both C–H bond activations by $\text{Pd}(\text{PH}_3)_2$. The same features are observed in the C–H bond activations by $\text{Pt}(\text{PH}_3)_2$. This is because the sp^2 orbital of C_6H_5 is at a lower energy than the sp^3 orbital of CH_3 , as has been discussed in the C–H bond activation by $M(\eta^2\text{-O}_2\text{CH})_2$. Also, the C_6H_5 π^* orbital contributes to the charge transfer from M to C_6H_5 , since it is at a rather low energy (3.4 eV) and can accept electrons from Pd and Pt. These features lead to the higher reactivity of benzene than that of methane, as will be discussed below in more detail.

Orbital Interaction in the C–H Bond Activation by $M(\eta^2\text{-O}_2\text{CH})_2$ and $M(\text{PH}_3)_2$. Because the orbital interaction diagram in the homolytic C–H bond activation by $M(\text{PH}_3)_2$ has been discussed previously,^{22,27c} we will briefly present the discussion. The important interaction is the charge transfer from the M d to the C–H σ^* orbital, as shown in Scheme 1. Since benzene

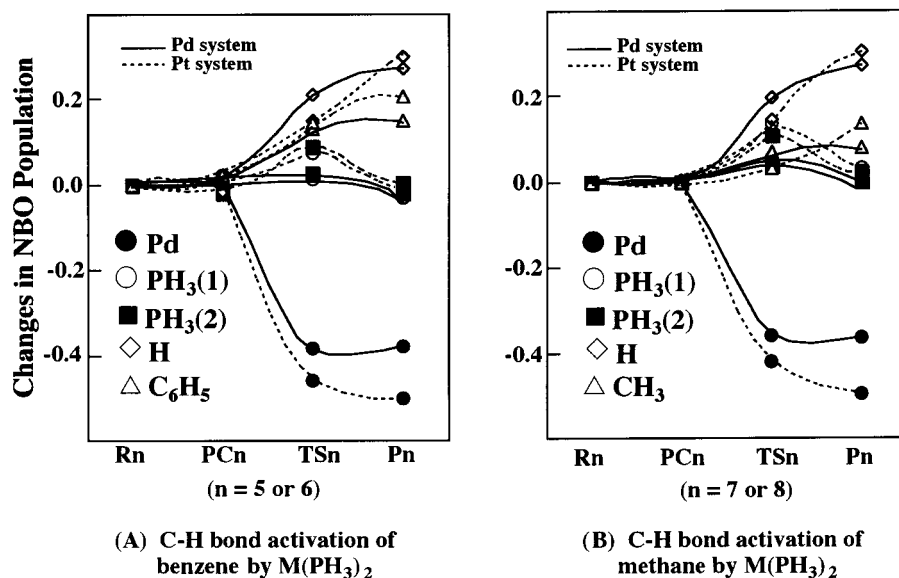
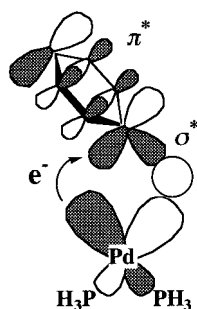


Figure 7. Population changes in the C–H bond activations of benzene (A) and methane (B) by $M(\text{PH}_3)_2$ ($M = \text{Pd}$ or Pt). A positive value represents an increase in population (vice versa). Solid lines represent population change for $M = \text{Pd}$, and dotted lines represent population changes for $M = \text{Pt}$.

Scheme 1



has a C–H σ^* orbital at a much lower energy (7.6 eV) than does methane (13.2 eV), the M d_π orbital forms the stronger charge-transfer interaction with benzene than that with methane. In addition, the benzene π^* orbital overlaps with the M d_π orbital, to provide a bonding interaction (Scheme 1). Thus, the homolytic C–H bond activation of benzene more easily occurs than that of methane by $M(\text{PH}_3)_2$. Actually, the electron population of C_6H_5 increases to a greater extent than that of CH_3 in the transition state, as discussed above.

The heterolytic C–H bond activation by $M(\eta^2\text{-O}_2\text{CH})_2$ exhibits completely different orbital interaction features. An important point is that $M(\text{II})$ has one empty d orbital at a rather low energy (–1.35 eV for Pd and –0.77 eV for Pt), as shown in Figure 8A. Here, we will show the orbital interaction in the Pd system, since the orbital interaction is essentially the same in Pt and Pd reaction systems. In **II**, this d_σ orbital interacts with the π and C–H σ orbitals of benzene, as shown in Scheme 2. In **TS1b**, two important interactions are observed, as shown in Figure 8B. In one (the next HOMO),⁷⁰ the HOMO of formate interacts in an antibonding way with the distorted π orbital of C_6H_5 , which undergoes σ – π mixing. This σ – π mixing easily takes place since the C–H σ orbital rises in energy by the bond-lengthening

and the back-bending of the C–H bond. In the other (the third HOMO), C–H σ orbital of benzene interacts with Pd d_σ orbital. However, both the next HOMO and the third HOMO still involve the bonding overlap between the sp^2 orbital of C_6H_5 and the H 1s orbital and the antibonding overlap between the O p_π orbital of formate and the H 1s orbital. To decrease this antibonding overlap, the C–H σ^* orbital must mix into the C–H σ orbital in a bonding way with the O p_π orbital of formate, as shown in Scheme 3. In the formate moiety, the O p_π orbital appears only in one O atom that is close to H but almost disappears in the other O atom. This feature arises from the mixing of two π orbitals, $\pi_{(\text{a1})}$ and $\pi_{(\text{b1})}$, which is induced by the positively charged H atom, as shown in Scheme 3. This type of orbital mixing was discussed by Imamura and Hirano.⁷¹ The significantly large positive charge of the active H atom means that the H 1s orbital contributes much less to the occupied space. Such small contribution also indicates that the mixing of the C–H σ^* orbital significantly occurs, as discussed above and in Scheme 3. All these orbital mixings are summarized, as follows: the sp^2 orbital of C_6H_5 interacts with the empty d_σ orbital of Pd, and the polarized π orbital of formate interacts with C–H σ^* orbital. The former interaction corresponds to the charge transfer from benzene to Pd, and the latter corresponds to the charge transfer from formate to the C–H σ^* orbital. These features are represented by a six-centered interaction shown in Scheme 4. Similar features are observed in the heterolytic C–H bond activation of methane, while one important difference exists between benzene and methane; in benzene, its π orbital also provides the bonding interaction with the Pd d_σ orbital, whereas methane does not have a good donating orbital. This is one of the important reasons for higher reactivity of benzene than that of methane.

Conclusions

The C–H bond activations of benzene and methane by $M(\eta^2\text{-O}_2\text{CH})_2$ and $M(\text{PH}_3)_2$ were theoretically inves-

(70) The HOMO does not involve any bonding interaction between benzene and Pd. This HOMO originates from the most stable π orbital of free benzene.

(71) Imamura, A.; Hirano, T. *J. Am. Chem. Soc.* **1975**, *97*, 4192.

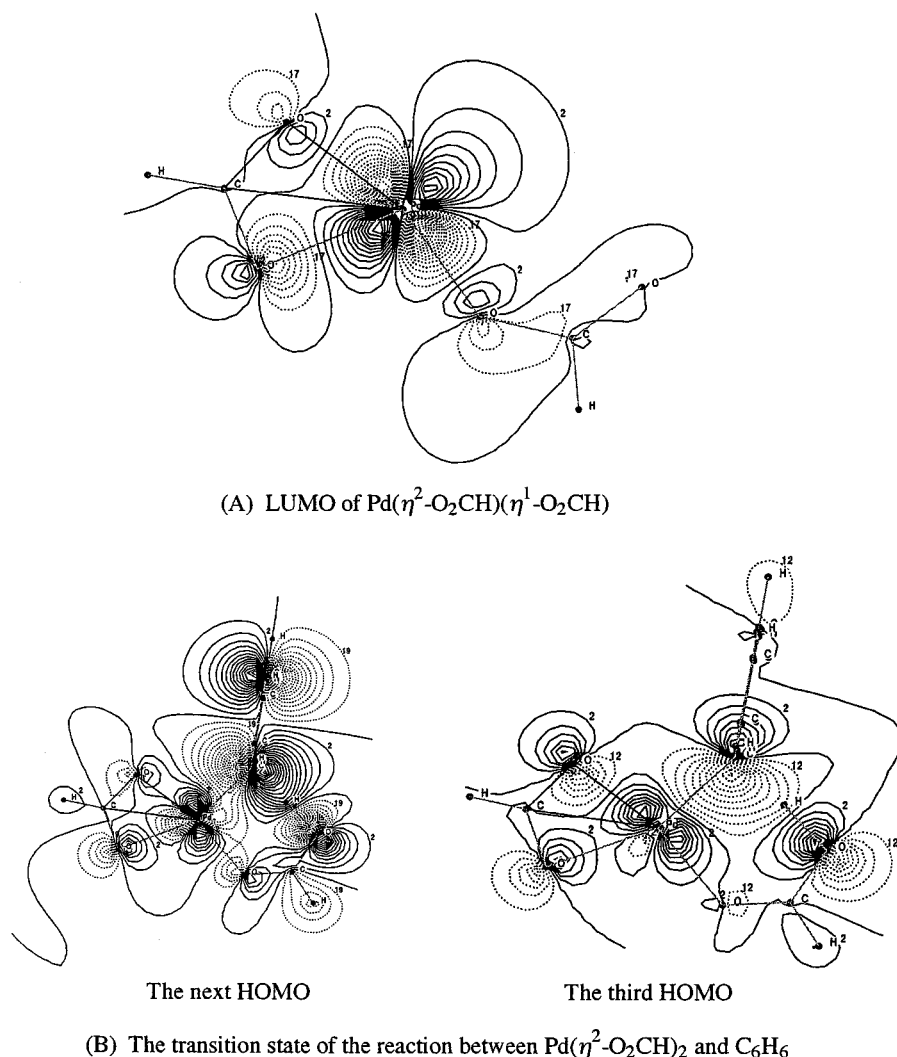
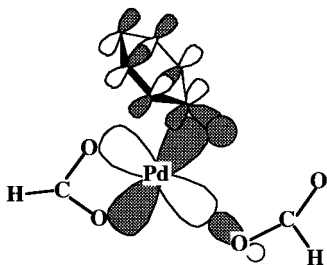


Figure 8. Contour maps of several important orbitals in the C–H bond activation of benzene by $\text{Pd}(\eta^2\text{-O}_2\text{CH})_2$. Contour values are ± 0.0250 , ± 0.0500 , ± 0.0750 , ± 0.0100 , and ± 0.1250 for the LUMO of $\text{Pd}(\eta^2\text{-O}_2\text{CH})(\eta^1\text{-O}_2\text{CH})$, ± 0.0125 , ± 0.0250 , ± 0.0375 , ± 0.0500 , and ± 0.0625 for the next HOMO, and ± 0.0250 , ± 0.0500 , ± 0.0750 , ± 0.0100 , and ± 0.1250 for the third HOMO.

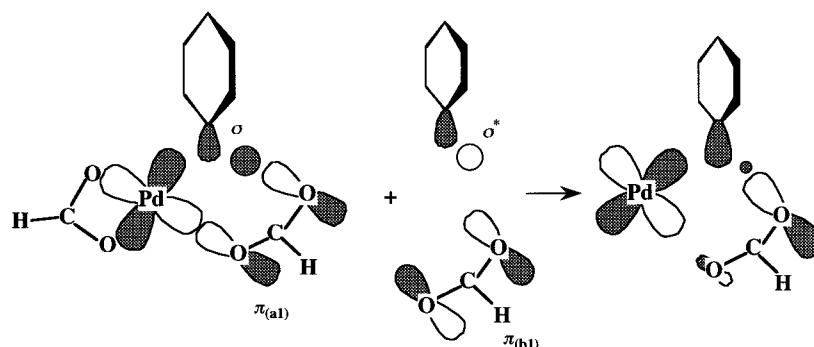
Scheme 2



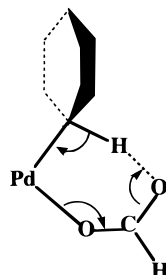
tigated with DFT, MP4(SDQ), and CCSD(T) methods. The C–H bond activation of benzene by $\text{M}(\eta^2\text{-O}_2\text{CH})_2$ proceeds through a van der Waals complex, the transition state leading to an $\text{M}(\text{II})$ –benzene complex, and the transition state leading to the final product, $\text{M}(\eta^2\text{-O}_2\text{CH})(\text{C}_6\text{H}_5)(\eta^1\text{-HCOOH})$. In the first transition state, benzene approaches M to replace one of the oxygen atoms of formate. In the second transition state, the C–H bond breaking and the O–H bond formation are underway, while the Pd–C bond formation has been nearly completed. An important feature of this transition state is a six-centered interaction in which the H atom is moving from benzene to formate while changing

into a proton. The C–H bond activation of methane by $\text{M}(\eta^2\text{-O}_2\text{CH})_2$ similarly takes place except that an intermediate, an $\text{M}(\text{II})$ –methane complex, is not as stable as the first transition state. The C–H bond activation of benzene by $\text{M}(\eta^2\text{-O}_2\text{CH})_2$ occurs with an activation barrier (E_a) of 16.1 kcal/mol and a reaction energy (ΔE) of -16.5 kcal/mol for $\text{M} = \text{Pd}$ and an E_a value of 21.2 kcal/mol and a ΔE value of -25.8 kcal/mol for $\text{M} = \text{Pt}$, where MP4(SDQ) values are given. The C–H bond activation of methane by $\text{M}(\eta^2\text{-O}_2\text{CH})_2$ takes place with an E_a value of 21.5 kcal/mol and a ΔE value of -8.3 kcal/mol for $\text{M} = \text{Pd}$, and an E_a value of 17.3 kcal/mol and a ΔE value of -13.3 kcal/mol for $\text{M} = \text{Pt}$. Thus, it should be reasonably concluded that (1) the C–H bond activation of benzene by $\text{Pd}(\eta^2\text{-O}_2\text{CH})_2$ easily occurs, as experimentally suggested, (2) the C–H bond activation of benzene by $\text{Pt}(\eta^2\text{-O}_2\text{CH})_2$ occurs less easily than that by $\text{Pd}(\eta^2\text{-O}_2\text{CH})_2$ because the intermediate, $\text{Pt}(\eta^2\text{-O}_2\text{CH})(\eta^1\text{-HCOOH})(\text{C}_6\text{H}_6)$, is too stable, (3) the C–H bond activation of methane by $\text{Pd}(\eta^2\text{-O}_2\text{CH})_2$ and $\text{Pt}(\eta^2\text{-O}_2\text{CH})_2$ can occur but less easily, and (4) $\text{Pt}(\eta^2\text{-O}_2\text{CH})_2$ is more favorable for C–H bond activation of methane than the Pd analogue.

Scheme 3



Scheme 4



The electronic process of the C–H bond activation by $M(\eta^2\text{-O}_2\text{CH})_2$ was investigated by electron distribution analysis. Important electron redistribution is that the M atomic population significantly increases while that of H remarkably decreases. From these results, it is reasonably concluded that the C–H bond activations of benzene and methane by $M(\eta^2\text{-O}_2\text{CH})_2$ are characterized to be heterolytic C–H bond fission in which the electrophilic attack of M to benzene or methane occurs concomitantly with the proton abstraction by the carboxylate ligand. This conclusion theoretically supports the experimental proposal.^{1d,31c}

The C–H bond activation of benzene by $M(\text{PH}_3)_2$ occurs with an E_a value of 26.5 kcal/mol and a ΔE value of 22.1 kcal/mol for $M = \text{Pd}$ and an E_a value of 17.1 kcal/mol and a ΔE value of –3.9 kcal/mol for $M = \text{Pt}$. The C–H bond activation of methane by $M(\text{PH}_3)_2$ takes place with an E_a value of 34.7 kcal/mol and a ΔE value of 31.5 kcal/mol for $M = \text{Pd}$ and an E_a value of 29.5 kcal/mol and a ΔE value of 7.1 kcal/mol for $M = \text{Pt}$. These results clearly indicate that the C–H bond activation by $\text{Pd}(\text{PH}_3)_2$ is very difficult. The reverse reaction occurs more easily than C–H activation in the Pd system. In these C–H bond activations, M d orbital population significantly decreases, while electron populations of H and R ($R = \text{C}_6\text{H}_5$ or CH_3) remarkably increase. These changes are consistent with our understanding that this reaction is characterized to be a typical oxidative addition, in other words, homolytic C–H bond fission.

The significant difference between $M(\eta^2\text{-O}_2\text{CH})_2$ and $M(\text{PH}_3)_2$ is interpreted in terms of C–H, M–H, and O–H bond energies and the interaction at the transition state. In the C–H bond activation by $M(\eta^2\text{-O}_2\text{CH})_2$, the M–O coordinate bond and the C–H bond are broken, but the M–R ($R = \text{C}_6\text{H}_5$ or CH_3) and O–H bonds are formed. In the C–H bond activation by $M(\text{PH}_3)_2$, the C–H bond is broken, but the M–H and Pd–R bonds

are formed. Since the O–H bond is much stronger than the sum of M–H and M–O bonds, the C–H bond activation by $M(\eta^2\text{-O}_2\text{CH})_2$ is more exothermic than that by $M(\text{PH}_3)_2$. In other words, the C–H bond activation by $M(\eta^2\text{-O}_2\text{CH})_2$ can be performed with assistance of the formation of the strong O–H bond. In the transition state of the C–H bond activation of benzene by $M(\eta^2\text{-O}_2\text{CH})_2$, the M d_σ orbital overlaps with the C–H σ and π orbitals of benzene to form the charge-transfer interaction, since the M d_σ orbital is at a rather low energy. In the C–H bond activation by $\text{Pd}(\text{PH}_3)_2$, the C–H σ* orbital of benzene must interact with the Pd d orbital, to form the charge transfer from the Pd d orbital to the C–H σ* orbital. However, this interaction is weak because the Pd d orbital is at a low energy.²⁴ Thus, the C–H bond activation by $\text{Pd}(\eta^2\text{-O}_2\text{CH})_2$ easily occurs, but the C–H bond activation by $\text{Pd}(\text{PH}_3)_2$ is difficult. In the Pt system, the C–H bond activation of methane by $\text{Pt}(\eta^2\text{-O}_2\text{CH})_2$ takes place more easily than that by $\text{Pt}(\text{PH}_3)_2$ for the same reasons. One exception is the C–H bond activation of benzene by $\text{Pt}(\eta^2\text{-O}_2\text{CH})_2$; this activation occurs less easily than that by $\text{Pt}(\text{PH}_3)_2$, because the intermediate, $\text{Pt}(\eta^2\text{-O}_2\text{CH})(\eta^1\text{-O}_2\text{CH})(\text{C}_6\text{H}_6)$, is too stable, as discussed above. The larger reactivity of benzene than that of methane arises from the fact that the M–C₆H₅ bond is much stronger than the M–CH₃ bond and that benzene has π and π* orbitals. The reasons for the stronger M–C₆H₅ bond are easily interpreted with simple molecular orbital theory.

Acknowledgment. Computations were carried out with an IBM SP2 machine at the Institute for Molecular Science (Okazaki, Japan) and an IBM RS6000/3CT workstation in our laboratory. This work is in part supported financially by the Ministry of Education, Science, Sports, and Culture of Japan through Grants-in-Aid on Priority Area “Molecular Physical Chemistry” (No. 403). B.B. thanks the Ministry of Education, Science, Sports, and Culture of Japan for a scholarship.

Supporting Information Available: Optimized geometry of $\text{Pd}_2(\text{C}_6\text{H}_5)(\eta^2\text{-O}_2\text{CH})(\mu^2\text{-O}_2\text{CH})_2(\text{SH}_2)$. Geometry changes in the C–H bond activations of benzene and methane by $\text{Pt}(\eta^2\text{-O}_2\text{CH})_2$, geometry changes in the C–H bond activation of benzene by $\text{Pt}(\text{PH}_3)_2$, and figures of vibration frequency calculations of **TSnb**, **n** = 1–4. This material is available free of charge via the Internet at <http://pubs.acs.org>.

OM000002S